UNIVERSITY OF LIFE SCIENCES AND NATURAL RESOURCES, VIENNA
DEPARTMENT OF FOOD SCIENCES AND TECHNOLOGY
INSTITUTE OF FOOD TECHNOLOGY - DIVISION OF FOOD BIOTECHNOLOGY

THE PRODUCTION, PURIFICATION AND ELECTROCHEMICAL CHARACTERIZATION OF ENGINEERED *BOTRYTIS ACLADA* LACCASE VARIANTS

Peter Herzog, BSc

To acquire the academic degree *Master of Science*

Supervisors

Priv.-Doz. Dr. Roland Ludwig
Dipl.-Ing. Dr. Roman Kittl
Dipl.-Ing. Stefan Scheiblbrandner

Vienna, 2015

Eidesstattliche Erklärung des Verfassers:

Ich erkläre ehrenwörtlich, dass ich die Arbeit selbständig angefertigt, keine anderen als die angegebenen Hilfsmittel benutzt und alle aus ungedruckten Quellen, gedruckter Literatur oder aus dem Internet im Wortlaut oder im wesentlichen Inhalt übernommenen Formulierungen und Konzepte gemäß den Richtlinien wissenschaftlicher Arbeiten zitiert, durch Fußnoten gekennzeichnet bzw. mit genauer Quellenangabe kenntlich gemacht habe. Diese Arbeit wurde in gleicher oder ähnlicher Form noch bei keinem/r anderen Prüfer/in als Prüfungsleistung eingereicht. Mir ist bekannt, dass die Verwendung unerlaubter Hilfsmittel rechtliche Schritte nach sich ziehen kann.

Peter Herzog, BSc

Wien, 30.11.2015

Acknowledgements

First of all, I wish to express my sincere gratitude to my supervisors DI Dr. Roman Kittl and DI Stefan Scheiblbrandner for giving me the opportunity to work on this project. Furthermore I would like to thank them for their guidance and for sharing their scientific experience.

I would also like to thank Erik Breslmayr MSc for his advice and for establishing a sound basis for my work.

Immeasurable appreciation is extended to Prof. Dr. Sergey Shleev for accommodating me in his scientific institution as well as for his endless support and inspiring expertise.

Further, I take this opportunity to thank Prof. Dr. Roland Ludwig and Prof. Dr. Dietmar Haltrich. I am extremely grateful and indebted to them for their sincere and valuable inspiration and encouragement extended to me.

This thesis is the product of a number of good-natured interactions and has benefited greatly from the assistance of all my colleagues and friends at the Department of Food Sciences and Technology at the University of Life Sciences and Natural Resources (Vienna) and the Department of Biomedical Science at the University of Malmö MAH.

Finally, I also extend my heartfelt thanks to my family without whom my academic education would have been a distant reality. Last but not least, I would like to dedicate this work to my lovely Martina.

"What we observe is not nature itself,
but nature exposed to our method of questioning."

Werner Heisenberg's *Physics and Philosophy: The Revolution of Modern Science (1958)*

Abstract

The exclusive combination of biochemical properties makes high redox potential laccases (HRPLs) an outstanding group of enzymes. As increasing knowledge about the enzyme is collected laccases present themselves as quite promising for their utilization in implantable biofuel cells.

For this application in particular, the absence of enzymatic activity at neutral pHs, the inhibition by modest chloride concentrations and the vulnerability to various compounds highlight the need for laccase engineering. Furthermore, the scientific community still lacks decent understanding of the electrochemical nature of the enzyme.
The recent developments of HRPL variants by directed evolution reported the successful improvement of biochemical properties. The creation of diverse mutational variants simultaneously presents a precious possibility to investigate the electrochemical features of laccases. A complex analysis could potentially draw a much anticipated connection between structure and electrochemistry and deliver novel information about the impact of mutational changes to the redox potential. Additionally, the correlation of laccase T1 midpoint potential (E_{T1}) and catalytic activity could be assessed.

Here I describe the third iteration of a directed evolution experiment on the *Botrytis aclada* laccase (BaLac) double mutant T383I I424M, the subsequent fermentation and purification of selected variants and an electrochemical evaluation of a set of ten BaLac variants by cyclic voltammetry (CV) and spectro-electrochemical redox titration.
The electrochemical analysis accomplished the determination of all T1 potentials and a decent approximation of T2/T3 potentials. Furthermore, full peak separation of the T2/T3 cluster potentials could be obtained for certain variants aided by an innovative CV setup. The results further suggested a relatively low degree of variation of potentials in the set of mutants.
This assessment could be the key to the rational design of redox variants of various multicopper oxidases in the future.

Kurzfassung

Die einzigartige Kombination biochemischer Eigenschaften macht Laccasen mit hohem Redox-Potential (HRPLs) zu einer außergewöhnlichen Gruppe von Enzymen. Während ständig neues Wissen über diese Enzyme generiert wird scheint klar zu werden, dass eine potentielle Anwendung von Laccasen in biologischen Brennstoffzellen sehr vielversprechend wäre.

Für diese Anwendung im speziellen, repräsentieren die Abwesenheit katalytischer Aktivität bei neutralem pH-Wert, die Inhibierung durch geringe Chlorid Konzentrationen und die Anfälligkeit gegenüber diversen chemischen Verbindungen die Notwendigkeit für Enzym Engineering. Des Weiteren mangelt es bis heute auch an einem angemessenem Verständnis der elektrochemischen Natur des Enzyms.
Die durch gerichtete Evolution kürzlich entwickelten HRPL Mutanten bestätigen die Möglichkeit der Verbesserung biochemischer Eigenschaften dieser Enzymklasse. Gleichzeitig bildet die Herstellung vielfältiger Mutanten des Enzyms auch eine wertvolle Möglichkeit zur Untersuchung der elektrochemischen Charakteristika von Laccasen. Eine vielschichtige Analyse könnte eine lang antizipierten Konnex zwischen Struktur und Elektrochemie des Enzyms schaffen und dabei Informationen über den Grad der Auswirkungen gentechnischer Veränderungen auf das Redoxpotential liefern. Außerdem wäre dadurch eine Aussage über den Zusammenhang des Potentials am katalytischen Zentrum T1 (E_{T1}) und der katalytischen Aktivität möglich.

In dieser Arbeit beschreibe ich die dritte Runde einer gerichteten Evolution der *Botrytis aclada* Laccase (BaLac) Doppelmutante T383I I424M, die anschließende Fermentation und Aufreinigung ausgewählter Varianten sowie die elektrochemische Untersuchung von zehn BaLac Mutanten mit cyclischer Voltammetrie (CV) und spektro-elektrochemischer Redoxtitration.
Die elektrochemische Analyse erreichte die Bestimmung aller T1 Potentiale sowie eine ausreichende Annäherung der T2/T3 Potentiale. Des Weiteren konnte für manche BaLac Mutanten eine vollständige Signaltrennung des T2/T3 Clusters mit Hilfe eines innovativen CV Setups erreicht werden. Die Ergebnisse der Messungen deuten auf eine relativ geringe Variation der Redoxpotentiale in der Sammlung der *BaLac* Varianten hin.
Die hier durchgeführten Untersuchungen könnten den Schlüssel zum rationalen Design von Redox-Varianten des Enzyms in Zukunft darstellen.

Contents

1. Introduction

After the first ideas of enzyme based biofuel cells were described in the early 1960s, research in the field was dynamically expanding ever since. Amongst the manifold ideas for implementation, the development of an implantable biofuel cell - serving as an internal and self-sustaining power source - remains to be the primary target of modern engineering advancements in this field (I. Ivanov et al., 2010). In this concept, blood, saliva or tears could serve as means to provide energy resources for various implantable biomedical devices such as cardiac pacemakers, insulin pumps, cochlear implants and biosensors. Due to its biological reaction mechanics and the nature of the physiological environment, the cell can only be operated inside a small window of operational requirements. In this regard, temperatures of 37 °C, a pH of 7.4 and high chloride concentrations (100-140 mM) have been identified as challenges to be overcome.

Several enzymes were assessed as possible biocatalysts for the application in biofuel cells. The family of multicopper oxidases (Pfam entry: PF00394) presents itself as a promising contender for the use as bio-cathodes. This is mainly reasoned by their ability to accept electrons at the expense of a reduction reaction of dioxygen to water, a reaction desirable for *in vivo* applications.
Within this family, fungal laccases are of special interest since they are characterized by a high redox potential, a broad substrate spectrum, good operational stability and the fact that they can reliably be produced in recombinant fermentation processes. Those properties led to the application of the laccase enzyme in distinct fields, comprising: bioremediation, waste water treatment, lignin degradation, polymer synthesis and food technology. These developments helped to increase the experience of working with the enzyme and resulted in a significant gain in knowledge.

The difficulties of the laccase enzyme to cope with temperatures of 37 °C, chloride inhibition and a neutral pH in particular raised the need for protein engineering approaches to tackle these drawbacks. In recent years, the scientific community achieved sustained success in improving the enzyme's resistance in these aspects. Diverse mutational variants were discovered and their improved enzymatic properties were characterized to draw conclusion about the complex structure-function relationship of the laccase enzyme.

Still, there is evident need to further increase the understanding of the enzymatic catalysis and the relation of its structure and function, also in order to be able to expand protein engineering approaches. Since the intra- and intermolecular transfer of electrons is the basis for the enzyme mechanics the detailed electrochemical investigation is regarded to be a key task of future work.

1.1. The laccase enzyme

1.1.1 Structural characteristics

Laccases (benzenediol:oxygen oxidoreductases, EC 1.10.3.2) are a member of the redox active "blue" multicopper oxidases (MCO) family. They are often also referred to as monophenoloxidases because of their substrate specificity. Commonly known copper containing enzymes like ceruloplasmin, bilirubin oxidase and ascorbate oxidase are relatives of the enzyme.

The laccase enzyme was originally identified in saps of the Chinese lacquer tree *Toxicodendron vernicifluum* in the late 19th century. This origin is still indicated by the name "laccase" (J. Needham et al. 1980). Till today, numerous representatives were found in fungi and plants predominantly, but recently also discovered in lichen, bacteria and insects (H. Forootanfar and M.A. Faramarzi, 2015). Nevertheless, laccases derived from basidiomycetes and ascomycetes represent the most highlighted examples in scientific research.

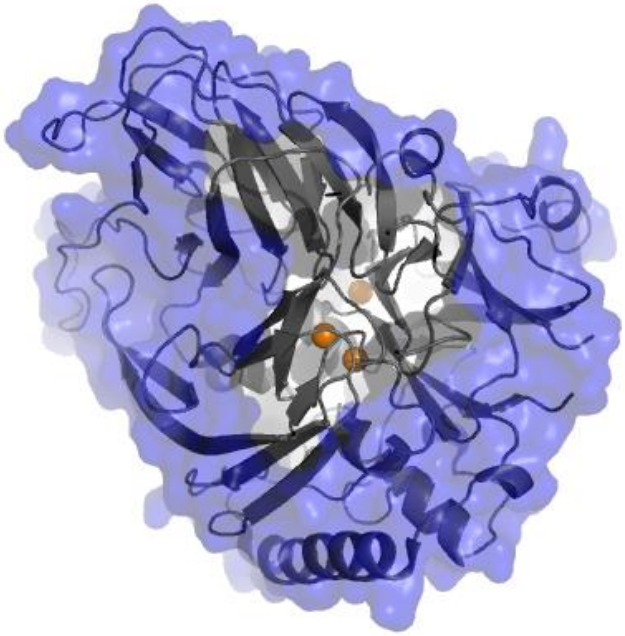

Figure 1: PyMOL 3D model of *Botrytis aclada* laccase derived from PDB crystal structure 3SQR. Although the active enzyme should naturally harbor four copper atoms (gold spheres) one is missing in the figure. The surface of the enzyme is indicated in transparent blue.

Although laccases can be found ubiquitously in nature and their structure and reaction mechanism is relatively similar, they still perform very diverse biological tasks. Laccases were reported to play an exclusive role in fungal lignin degradation as well as in the lignin formation of higher plants. In addition to that, laccases of phyto-pathogenic fungi can mediate the neutralization of tannins,

phytoalexins and phytoanticipins and therefore allows the fungus to counter the plant's defense system. In *E. coli*, the laccase enzyme CueO is reported to facilitate copper homeostasis (S.A. Roberts et al., 2002).

The majority of fungal laccases are moderately glycosylated, monomeric exo-enzymes. Their structure comprises three cupredoxin-like domains, a scaffold that is arranged in a greek key beta-barrel motif and typical for copper interaction in proteins. Most fungal laccases are characterized by a molecular weight of 60-70 kDa, a carbohydrate moiety of generally 10-20% that is high in mannose and a theoretical p*I* of less than 4.0. Actual p*I* values can even be lower (O.V. Morozova et al., 2007).

The responsibility for the relatively wide array of possible substrates: (poly) phenols, (poly) amines, aryl diamines and inorganic ions are amongst them; may root in the distinctive architecture of the binding pocket of the enzyme. It features a relatively large accessible area and allows for diverse chemical interaction with the substrate (S. Riva, 2006).

The catalytic nature of the redox-active laccase enzyme is determined by its highly conserved coordination of four copper atoms in the active site. These copper atoms are arranged in two centers: a single mononuclear "blue" copper (T1 site) and three copper atoms coordinated to a tri-nuclear copper cluster TNC (T2/T3 site). These positions are separated by approximately 13 Å (F. J. Enguita et al., 2003). Furthermore, the copper atoms are classified by their physico-chemical properties by means of EPR and spectroscopy and perform different duties in the catalytic reaction.

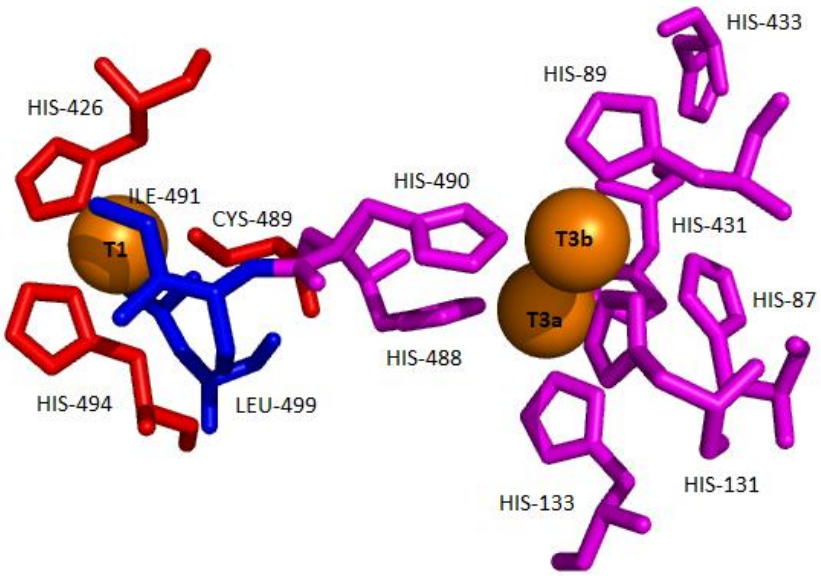

Figure 2: PyMOL 3D model of the catalytic center of the laccase enzyme of *Botrytis aclada* modified from Johannes Führer (J. Führer, 2015, unpublished). The copper atoms are depicted as golden spheres. The T1 is coordinated by three amino acid residues (red, His494, His426 and Cys489). Leu499, found as Met499 or Phe499 in other laccases as well, and highly conserved Ile491 (blue) act as axial ligands. The tri-nuclear cluster (lacking one copper in the figure) is coordinated by the imidazoles of four histidine tandems (pink).

The T1 copper is characterized by producing a typical “blue” absorption signal at circa 600 nm and a weak parallel splitting in EPR analysis. It is situated in close proximity of the site of substrate oxidation and coordinated by two histidine imidazoles and the sulfhydryl group of cysteine in a planar triangular fashion. An additional phenylalanine, leucine or methionine residue assists in copper binding and is also used to categorize laccases from different origin in high-, medium-and low redox potential laccases, respectively. However, the direct ligand environment of the T1 appears to have only a minor influence on the T1 redox potential (F. Xu et al., 1999). For fungal laccases, values of up to E_m = +790 mV vs NHE are reported.

The tri-nuclear cluster T2/T3 comprises a single T2 copper and two T3 copper, often referred to as Cu3a and Cu3b. The optical analysis of characteristic absorption spectra of the T2/T3 site is problematic since its peak is situated at 330 nm and often superimposed by background signal of the protein. Thus, the differentiation of copper species in the cluster relies on the dissimilar behavior in EPR analysis where, in contrast to the undetectable T3, the T2 displays a discrete spectrum (L. Quintanar et al., 2005). A conserved arrangement of four His-X-His motifs is ligand for the conserved coordination of the copper atoms in the T2/T3 cluster

1.1.2 Catalysis

The high redox potential of the T1 site of laccases endows the enzyme with the ability to accept electrons from a wide range of reducing substrates. This variety can even be expanded by coupling the redox reaction with so called redox mediators. In a cascade of electron exchange, those components are directly oxidized by the laccase and in return can mediate the chemical oxidation of other compounds. This principle allows to access substrate that would be unavailable otherwise still at the expense of dioxygen as final electron acceptor. In general, laccases are capable of oxidizing compounds with an ionization potential lower or similar to their T1 potential. The redox mediator system might be an exception to this principle, though.

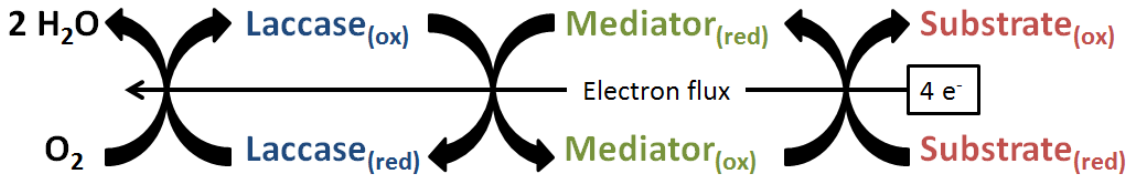

Figure 3: Scheme of the Laccase Mediator System (LMS). Electrons drawn from a substrate are transferred onto a mediator, to the mediator and the laccase subsequently and are finally used to reduce dioxygen to water in a 4 electron reaction. Note that all electron transfers are distinct reactions that can occur locally and timely separated.

The LMS is assumed to play a vital role in the interaction of laccases with lignin, where presumably only small molecules can enter the dense framework of the lignin polymer. A prominent mediator extensively utilized in the LMS is ABTS (2,2'-azino-bis (3-ethylbenzothiazoline-6-sulphonic acid)). It

also is the colorimetric agent in most biochemical enzyme assays. Mediators that represent a more native substrate for the enzyme are for instance 2,6-DMP (2,6-Dimetoxyphenol) and guaiacol. The catalytic properties of the same laccase can widely vary for different kinds of substrates and depends on the chemical nature of the substrate.

The one electron oxidation of a substrate molecule is initiated by the T1 copper collecting a single electron from a substrate. The subsequent transport of electrons to the T2/T3 site is thought to be assisted by a Cys-2His pathway. After overcoming the 13 Å distance, the copper-cluster-bound O_2 can be reduced to H_2O (E.I. Solomon et al., 1996). Here it should be stated that research still lacks a consensus theory of electron transport between the T1 and T2/T3.
This enzymatic cycle of dioxygen reduction relies on the activated, fully oxidized state of the laccase enzyme. It is then characterized by the four coppers being present in a bivalent cationic state (Cu^{II}). This state is commonly known as native intermediate and represents an oxygen radical connecting the three T2/T3 coppers. Upon electron influx of four electrons, all coppers are reduced to a monovalent cation and oxygen is removed from its binding pocket in the TNC during its reduction. A reduced form of the active site is now established, that will transform to a short-lived peroxide intermediate upon loading with dioxygen and can again develop the native intermediate. The oxidized and catalytically irrelevant "resting" form can evolve from the native intermediate (S. Shleev et al., 2006).

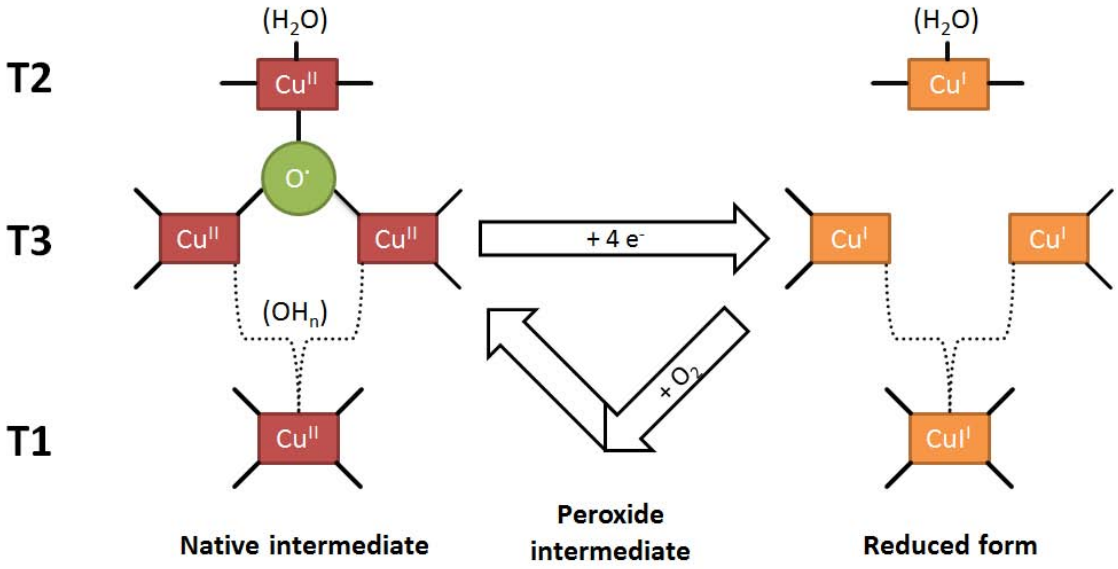

Figure 4: Scheme of the transformation of copper coordination of the laccase's active site during the catalytic cycle. The four Cu^{II} units are interacting with an oxygen radical at the T2/T3 site and are reduced to monovalent Cu^{I} cations upon retrieval of electrons during the change from the "native intermediate" state to the "reduced form". This transition is reversed when oxygen is supplied and creates a "peroxide intermediate" state.

Most laccases are inhibited by small nucleophilic anions such as halides, pseudo-halides, carbonates, sulfides or cyanides. Experiments with fluoride and chloride showed impairing effects on the catalysis in particular. It is thought that these components compromise the redox potential of the T2/T3 site (B.R.M. Reinhammar et al., 1971) or directly block the electron transport by competitive binding to the copper entity (F. Xu, 2001). In addition to that, the cyanide ion is used in various studies as a means to deplete copper from the active site in proves that inhibitors can also cause the removal of copper from the enzyme.

For the majority of fungal laccase species, the pH is crucial for their stability and catalytic activity. They prefer an acidic milieu that generally ranges from pH 3.5 to 5.0. It is assumed that the accumulated binding of hydroxyl ions and the resulting drop in redox potential at the T2/T3 site is responsible for the loss of activity at higher pHs (F. Xu, 1997).

1.1.3 Electrochemistry

The redox potentials of the laccase's T1 site can be found between 0.43 V and 0.79 V vs NHE. Still, values for laccases from basidiomycete origin display the highest potentials. Currently, there is little information about the potentials and other electrochemical properties of the T2 and T3 site yet (O.V. Morozova et al., 2007). For the related bilirubin oxidase (BOx) enzyme potentials of the T1 site (E_{T1}) are comparable to those of laccases, were assessed to be 0.7 V and are coinciding with catalytic waves of oxygen bio-electroreduction. $E_{T2/T3}$ could also be obtained for BOx in experiments and were reported to be approximately 0.4 V vs NHE (P. Ramírez et al., 2008).

As has been described previously, the type of non-conserved axial ligand of the T1 copper, namely phenylalanine, leucine and methionine determine the classification of E_{T1} potentials but seem to have limited influence when been exchanged in mutational experiments (P. Durão et al., 2006). It is assumed that their major purpose is to maintain a hydrophobic surrounding at the Cu1. A substantial influence on the E_{T1} is attributed to the second coordination sphere of the T1. The positions 292-297, 419-424 and 441-445 in the neighboring loops were subject to mutational alterations that resulted in a change of T1 potentials of up to 250 mV (E. Osipov et al., 2014).

Laccase enzymes that are located on electrodes in electrochemical experiments are thought to have a unique orientation that is dependent on the electrode material and possible modification.
When exposed to carbon surfaces, the enzyme is set in a fashion that the T1 site is remote to the electrode. The distance is reported to be less than 10 Å and allows for direct electron tunneling to the Cu1 and subsequent native intramolecular transfer to the T2/T3.

The laccase orientation is reversed for (modified) gold surfaces where the T2/T3 center is adjacent to the electrode, still able to directly receive electrons from the surface. The relay of electrons to the T1 site might be hindered or below biological relevant levels though (P. Ramírez et al., 2008).

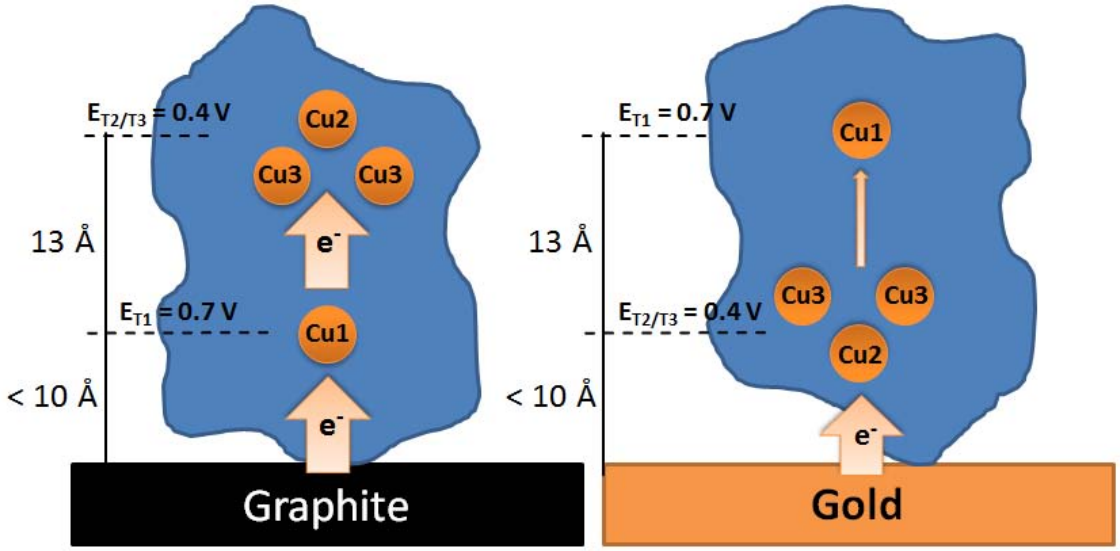

Figure 5: proposed mechanism of direct electron transfer (DET) to blue mutlicopper oxidases on carbon (left) and gold (right) electrodes. Different orientation of the enzyme results in different electrochemical properties.

Assuming that the current estimations of redox potentials of both redox centers are accurate, the natural IET would contain an uphill transport step. Hence it is likely that electrons accepted at a potential of circa 0.7 V (T1) are transferred against their exergonic ambition to a potential of circa 0.4-0.5 V (T2/T3). Furthermore, it could be possible that actual redox states in the catalytic cycle are not gathered by the measurement since the T2/T3 is trapped in the more stable resting form (S. Shleev et al., 2012).

It has been discussed recently that the simultaneous addressing of several redox centers in oxidoreductases should be possible in experiments such as cyclic voltammetry. The natural electrical connection of the two centers in laccase should deliver sufficient currents for analysis. A similar principle was subject for debate in the case of FeS clusters in fumarate reductase (A. Sucheta et al., 1993). Here, an autonomous step of electron transport should include just a single electron. This was justified in experiments consistent with signals expected from Marcus-DOS theory of electron transfer. Nevertheless, the actual mechanics of electrical interaction are still yet to discover. Electrochemical assessments that are performed in the presence of soluble redox mediators of a proper potential range could circumvent undesired laccase orientations and directly wire the T1 site.

1.2. The *Botrytis aclada* laccase

The plant pathogen *B. aclada* belongs to the division of ascomycetous fungi and is commonly known to cause neck rot in stored crops such as onions (M.I. Chilvers and L.J. du Toit, 2007).

Its laccase enzyme, often referred to as “BaL” or “BaLac”, contains 561 amino acids that account for a theoretical molecular weight of 61.6 kDa. The maturely glycosylated enzyme was found to have a molecular weight of approximately 110 kDa though, one of the highest glycan moieties in the group of laccases. Furthermore, the enzyme displays a tendency for the formation of dimers. Its p*I* was determined in experiments to be approximately 2.4. An x-ray structure analysis of the crystalized enzyme was successfully performed and is archived as entry 3SQR in the PDB (E. Osipov et al., 2014).

BaLac features characteristics that make it remarkably interesting for biotechnological applications. Firstly, although classified as medium-potential laccase by its axial leucine Cu1 ligand, it is endowed with a high potential of E_{T1} = 0.72 V. In addition to that, the enzyme is hardly inhibited by chloride (I_{50} = 1.4 M). The resistance to modest chloride concentrations is a rare quality for a laccase and vital for the use in various applications. Furthermore, this laccase shows a favorable catalytic performance for the majority of common substrate with low K_m values. The recombinant expression of BaLac in *Pichia pastoris* has been successful in various approaches. A straight-forward fed-batch fermentation process yielded activities of 53 300 U L^{-1} and protein concentrations of 517 mg L^{-1} in a 97 h protocol (R. Kittl et al., 2012). Last but not least, the exclusive set of advantages that can be combined with the previously described possibilities for direct electron transfer (DET) make the laccase a promising candidate for the application in biofuel cells in particular

Like the majority of laccase variants, the laccase of *B. aclada* struggles to retain stability when being exposed to higher temperatures, to detergents, fatty acids, metal ions etc. Also, the display of limited to no activity at neutral/basic pHs is an obstacle to its further exploitation.
Modern protein engineering approaches were reported to evolve enzymes in a way that their shortcomings are diminished. The two factors of pH dependent activity and thermal stability (reflecting overall stability and resistance to various chemical compounds) might be extraordinarily suitable for protein engineering efforts to improve the laccases fitness.

1.3. Directed evolution

Directed evolution (DE) is a potent approach in modern protein engineering to alter or optimize specific properties of a protein towards a defined target. This method relies on submitting a gene to iterative cycles of mutagenesis, screening and gene amplification therefore imitating the natural process of evolutionary selection on a laboratory scale.

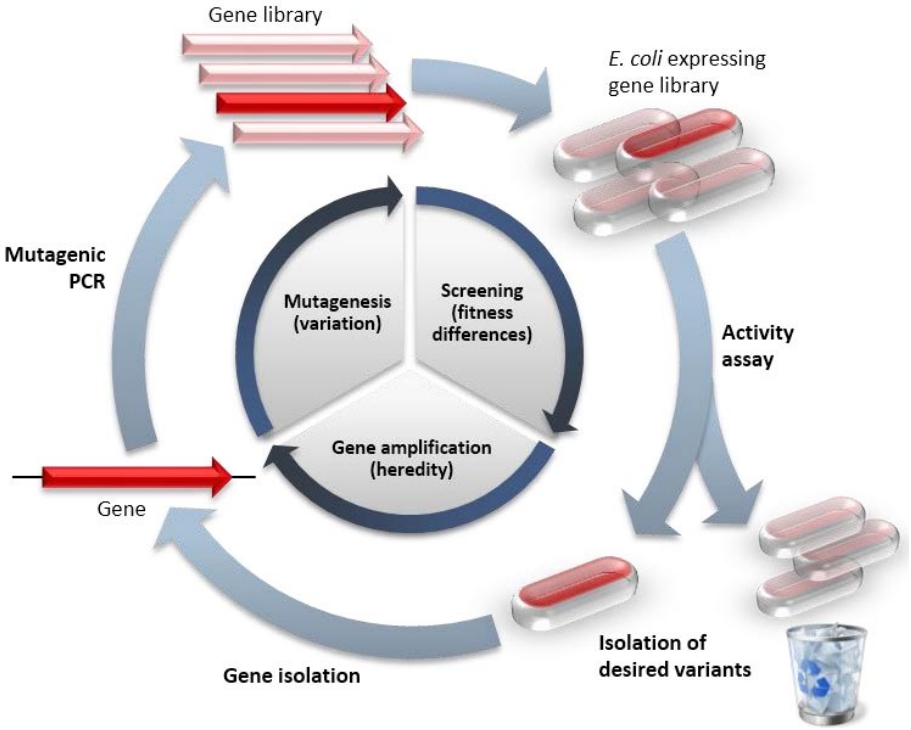

Figure 6: Scheme of the cyclic sequence of mutagenesis (variation), screening (survival of the fittest) and gene amplification (heredity) of directed evolution. By curtesy of Thomas Schafee (T. Schafee, 2015)

The variation of genetic content in the target gene is generally accomplished by random mutagenesis techniques like error prone PCR or gene shuffling that create a genomic library. The phenotypical performance of a distinct variant is assessed in a subsequent screening mimicking an environment to favor improved variants. After isolation, the mutational changes responsible for the improved functionality are elucidated and inherited. The variant can now be subjected to a next round of DE

Enzymes are often templates for DE engineering. They can be evolved towards variants with improved catalytic properties, altered resistance to inhibitors, increased thermal stability or changed substrate specificity. One important advantage of DE is that it is not essentially reliant on information about the structure-function relation, which generally limits the output of rational design approaches. This feature makes it convenient for complex enzyme studies. Nevertheless, the success of DE setups vastly depends on high-throughput screening methods (D. Mate et al., 2013).

1.4. Laccases in biofuel cells

Biofuel cells operate on the general principle of coupling an exergonic tandem of redox reactions. In contrast to batteries they rely on an influx of fuel, respectively substrate. The enzymatic setting of cells often features a combination of oxidases such as glucose oxidase (GOx) on the anode and multicopper oxidoreductases on the cathode of the cell. In the redox cycle, GOx can provide electrons to the system by bio catalytic oxidation of glucose. These electrons become available for enzymes like laccases which utilize them for the reductive conversion of dioxygen to water (R.A. Bullen et al., 2006). The use of glucose, molecular oxygen and generation of water as a main product present clear advantages of laccases in the scope of their use in biomedical applications.

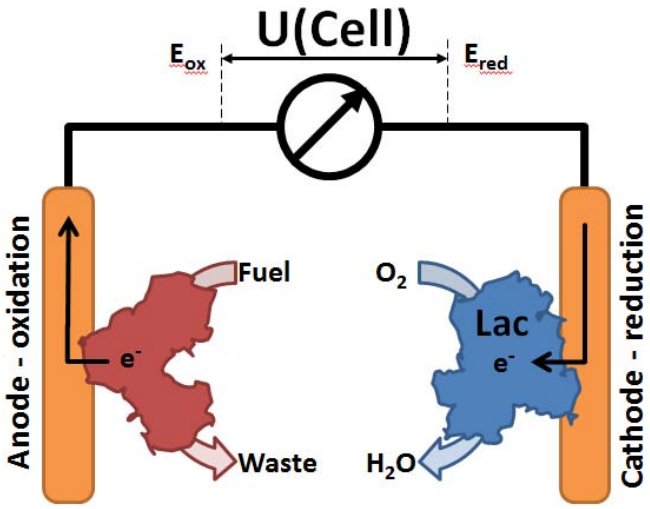

Figure 7: Schematics of a biofuel cell applying laccase (blue, Lac) as a biocatalytic cathode

This balance of bio-electrochemical processes supplies electrical power that is proportional to the current (dependent on the number and rate of parallel reactions) and the cell voltage (dependent on the difference in enzyme redox potentials). In this regard, the combination of GOx (Em = - 0.1 V) and high redox potential laccases HRPL (Em = + 0.7 V) would be valuable for the cell's power output. Note that negative E_m values indicate a driving force to release electrons, positives values to accept electrons respectively.

The effective immobilization of enzymes on electrodes and suitable means to guarantee decent electron transfer to and from the enzyme represent essential prerequisites for enzymatic biofuel cells. Amongst other approaches, the modification of carbon electrodes with various nanotube/nanoparticle species and the formation of self-assembled thiol monolayers like the 3-mercaptopropionic acid (MPA) modification of gold electrodes are thought to simultaneously fulfill both requirements whilst increasing the effective surface of the electrode. Still, the often described DET between laccases and electrodes is a relevant element for its applicability.

1.5. Aim of this work

This master thesis aimed at increasing our understanding of the structure-function relation of laccases in the scope of exploring and redefining structural parts that may contribute to its enhanced utility.

The performed directed evolution approach intended to target both the pH profile and the thermal stability of the previously discovered enzyme variant BaLac T383I I424M which served as a template for the third iteration of this protein engineering approach. The screening stage was designed to identify circa ten improved variants harboring preferably one additional mutation. A consecutive fermentation and purification procedure of the most promising variants was to be performed to yield sufficient amounts of pure enzyme for characterization.

In addition to that, it was decided to evaluate the electrochemical potentials of a set of variants in an extensive electrochemical analysis. This group of BaLac variants originated from several rational, semi-rational and random mutagenesis setups that were performed by different coworkers in recent years. Hence, the source of genetic alteration and its phenotypic effect were quite diverse and included different combinations of mutations as well. This evaluation again addressed the connection of the enzyme's structure and function, here focusing on its electrochemical features. It was performed to support statements about the degree of influence on potentials and the possible connection to catalytic performances of certain variants. It is fair to say that this electrochemical study may represent one of the largest in this field of multicopper oxidases.

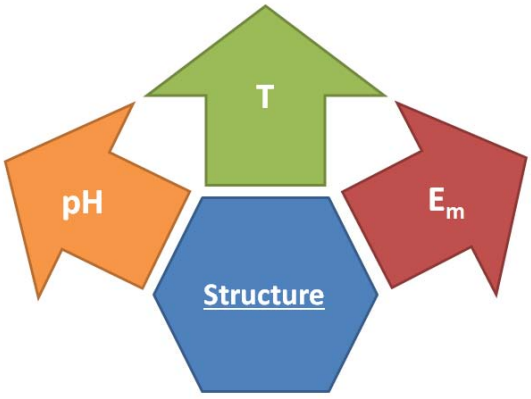

Figure 8: Schematics to summarize the three functional aspects that are in the focus of this work and root in the structure of the laccase enzyme: the catalytic pH profile (yellow, pH), the thermal stability (green, T) and electrochemical redox (midpoint) potential (red, E_m).

Still, the contribution to the development of a *B. aclada* laccase variant suitable for the use in biomedical applications remained to be the ultimate goal of this scientific project.

2. Materials and Methods

2.1. Genetic engineering

2.1.1. Primers

For the standardized molecular biology procedures in the directed evolution approach such as error-prone PCR, colony PCR and DNA sequencing, a selection of primers listed below was used.

Table 1: List of standard primers used for cloning and sequencing

Primer name	5' to 3' sequence
pGAPfw2	5'- CCCAATTTTGGTTTCTCCTGAC -3'
3ZLHGAP1rev	5'- GGCGCTATTCAGACCTCTTC -3'
3BaL (T383Irev)	5'- TGA GAA TGG TTG GGG AGC TCC -3'
3AOX	5'- GCAAATGGCATTCTGACATCC -3'
pJET1.2fw	5'- CGACTCACTATAGGGAG -3'
pJET1.2rev	5'- ATCGATTTTCCATGGCAG -3'

Primer solutions of pGAPfw2, 3 ZLHGAP1rev, 3BaL (T383Irev) and 3AOX were ordered from VBC Biotech (Austria) for previous experiments and diluted with sterile uHQ-H_2O to concentrations of 100 pg μL^{-1} for storage at -20°C. pJET1.2 forward and reverse primers came alongside the original CloneJET PCR Cloning Kit (Thermo Fisher Scientific, Waltham, MA, USA) in 10 µM aqueous solution. For the use in PCRs and DNA sequencing, primer stocks were prepared as 1:10 dilutions.

2.1.2. Vectors

The gene expression vector pGAPZA (Invitrogen, Carlsbad, CA, USA), endowed with the constitutive glyceraldehylde-3-phosphate dehydrogenase (GAP-DH) promotor, was chosen for recombinant protein expression of the functional *Botrytis aclada* laccase variants in *Pichia pastoris* X-33 cells (Invitrogen).

The pGAPZA vector, derived from the methanol inducible pPICZ vector generation, is further equipped with a pUC origin of replication, allowing it to be amplified in prokaryotic hosts like *Escherichia coli.* Furthermore, the vector harbors the *Sh ble* gene. Its expression product can neutralize the antibiotic Zeocin (Invitrogen) and therefore permit the use as a selection marker.

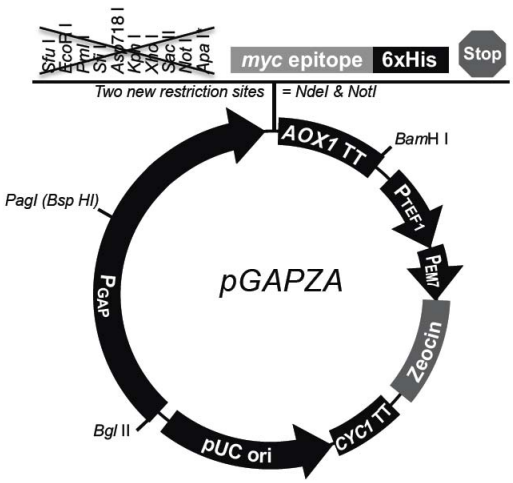

Figure 9: Vector map of the modified pGAPZA vector including digestion sites. By curtesy of E. Breslmayr, 2015

To elucidate alterations in the sequence of the laccase gene template, the pJET1.2/blunt Cloning Vector (Thermo Fisher Scientific) served as a backbone to carry the inserts of interest. This vector is endowed with blunt-ended DNA termini, allowing a straight forward insertion of PCR products created with proof reading DNA polymerases. Products obtained by PCR reactions with non-proof-reading enzymes, such as *Taq*-polymerase, can be treated with a blunting enzyme prior to ligation with the vector. This vector system is equipped with a positive selection system, a lethal restriction enzyme gene under the control of the lacUV5 promotor that is neutralized upon insertion of a DNA insert into the cloning site. Furthermore, the pJET1.2/blunt cloning vector contains a pMB1 replicon and the selection marker gene *bla* which confers resistance to ampicillin when expressed.

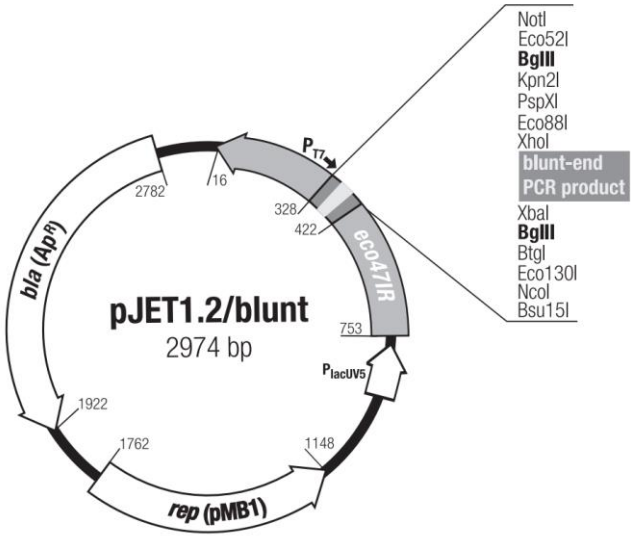

Figure 10: Vector map of the pJET1.2/blunt cloning vector with MCS noted

2.1.3. Host organisms

As a DNA template for the random mutagenesis approach, the wild type *Botrytis aclada* laccase gene was inserted into a pGAPZA vector backbone. This vector was genetically engineered to have an *Nde*I and *Not*I restriction site inserted, in return the *Sac*I restriction site, originally situated in the multiple cloning site, was removed. This vector construct was referred to as BAGANSN.

The *Escherichia coli* strain NEB 5-alpha (New England Biolabs, Ipswich, MA, USA) served as the host organism for the creation of the error prone library. The organisms genotype can be specified as followed: *fhuA2_(argF-lacZ)U169 phoA glnV44 _80_(lacZ)M15 gyrA96 recA1 relA1 endA1 thi-1 hsdR17.*

For the recombinant expression of laccase variants in small scale fermentation and for the high-throughput-screenings of the variant library the genes were transformed into electro-competent *Pichia pastoris* X-33 cells (Invitrogen).

2.1.4. Restriction enzymes

The nucleases used were all acquired from Thermo Fisher Scientific (USA). In the case of the pJET blunting enzyme, which was used in cloning experiments to determine mutation rates of error prone PCR reactions, the enzyme solution came with the CloneJET PCR Cloning Kit. Unless stated otherwise, all digestion reactions were carried out according to the standard protocols provided by the supplier.

Table 2: List of endo- and exonucleases used; given their restriction site and preferential buffer usage

Enzyme	Restriction site	Buffer
*Dpn*I	5´…G m6A ▼ T C…3	Tango
*Not*I	5´…C A ▼ T A T G…3´	O
*Nde*I	5´…G C ▼ G G C C G C…3´	O
*Pag*I (*BspH*I)	5´…T ▼ C A T G A…3	O
pJET blunting enzyme	exonuclease*	pJET Reaction Buffer

***** the site of exonuclease reaction is solely dependent on the sequence of the inserts

2.1.5. DNA polymerases

The Mutazyme® II DNA Polymerase, part of the GeneMorph II Random Mutagenesis Kit (Agilent, Santa Clara, CA, USA), is a blend of two thermostable error prone DNA polymerases and is designed for PCR reactions in random mutagenesis approaches. It is, as a member of the *Taq*-polymerase

family, derived from the thermostable bacterium *Thermus aquaticus* and lacks proof-reading activity. This enzyme was engineered based on Mutazyme® I DNA polymerase to provide useful mutation rates with reducing the mutational bias.

Go*Taq*-polymerase G2, delivered by Promega (Madison, WI, USA), is another representative of the *Taq*-polymerase family. Although the error rate during PCR reaction is reported to be relatively low when optimal conditions can be maintained, the enzyme is not fit for use in high quality DNA treatment and thus, was used for gene amplification only.

2.1.6. Kinases and ligases

FastAP (Thermo Fischer Scientific) is a novel temperature sensitive Alkaline Phosphatase which catalyzes the release of both 5'- and 3'-phosphate entities from various substrates such as DNA, RNA or proteins. It is designed to dephosphorylate all kinds of DNA ends in order to prevent undesirable (re)ligation of vector termini.

For vector ligation, the T4-DNA Ligase enzyme (Promega) was used. It catalyzes the connection of two DNA strands between the 5'-phosphate and the 3'-hydroxyl groups of adjacent nucleotides. It is reported to function with DNA substrates of 5' or 3' sided DNA overhangs or such of blunt ended configurations.

2.2. Chemicals

All buffers and solutions were prepared with ultra-high quality water (uHQ-H_2O) with a resistivity of at least 16 MΩ cm. All chemicals used were of reagent-grade purity.

- 100 mM 2,6-DMP-solution (40x stock):

154,2 mg	2,6-Dimethoxyphenol (FLUKA, St. Gallen, Switzerland)
10 mL	uHQ-H2O

This stock solution was stored for further use at -20 °C in aliquots of 1.0 ml.

- 10 mM ABTS-solution:

54.9 mg	ABTS diammonium salt (Amresco, Solon, OH, USA)
10 mL	uHQ-H_2O

ABTS solution was not stored but prepared freshly as often as possible.

2.3. Media

Table 3: List of cultivation media for bacteria and yeast

Label	Abbrevation	Organism
Luria-Broth*	LB	*Escherichia coli*
Super optimal broth – catabolite repression	SOC	
Yeast extract-Peptone-Dextrose*	YPD	*Pichia pastoris*
Buffered-Yeast extract-Peptone-Dextrose	BYPD	
Buffered-Minimal-Glycerol	BMG	
Yeast Nitrogen Base	YNB	
Fermentation Basal Salt Medium	FBSM	
Pichia Trace Metal Salts	PTM_1	

* media could be supplemented with antibiotic for selection

- Super optimal broth medium SOC (New England Biolabs):

2 %	Vegetable peptone
0.5 %	Yeast extract
10 mM	NaCl
2.5 mM	KCl
10 mM	$MgCl_2$
10 mM	$MgSO_4$
20 mM	Glucose

Autoclaving was then carried out at the standard conditions of 121 °C for 15 min prior to cooling the media at 60 °C in a water bath.

- Luria-broth (LB) low salt:

10 g	Peptone from casein (Sigma-Aldrich, St. Louis, MO, USA)
5 g	Yeast extract (Carl Roth, Karlsruhe, Germany)
5 g	Sodium chloride (Sigma-Aldrich)
1 L	RO-H_2O

For the preparation of agar plates, agar-agar was added as stated:

15 g	Agar-Agar Kobe I (Carl Roth)

Autoclaving was then carried out at the standard conditions of 121 °C for 15 min prior to cooling the media at 60 °C in a water bath. For the preparation of selective medium, either Zeocin (LB-ls Zeo^+) or Ampicillin (LB-ls Amp^+) was then added to the well-tempered solution to reach a concentration of 25 mg L^{-1}.

- Yeast peptone dextrose (YPD):

20 g	Peptone from casein
10 g	Yeast extract
4 g	D-Glucose (Merck, Darmstadt, Germany)
1 L	RO-H2O

For the preparation of agar plates, agar-agar was added as stated

15 g	Agar-Agar Kobe I

Autoclaving was then carried out at standard conditions prior to cooling the media at 60 °C in a water bath. For the preparation of selective medium, Zeocin was then added to the well-tempered solution to reach a concentration of 100 mg L^{-1}.

- Buffered yeast peptone dextrose (BYPD):

Compared to the preparation of the YPD medium, the same amounts of compounds were prepared with just 900 mL of uHQ-H_2O. This mix was then autoclaved before 100 mL of sterile 1 M KPP-buffer of desired pH were added to yield a final concentration of 100 mM buffer.

- Buffered minimal glycerol (BMG) medium:

15 g	Agar-Agar Kobe 1
778 mL	uHQ-H_2O

Autoclaving was then carried out at standard conditions and followed by adding the stated sterile solutions in a laminar flow hood.

100 mL	KPP-buffer pH 6.5
100 mL	10 % Glycerin-solution (10x GY)
100 mL	10x YNB-solution

The following sterile filtered solutions were added

10 mL	20 mM ABTS-solution
10 mL	10 mM Cu(II)SO_4-solution
2 mL	500x Biotin-solution

- 10x GY stock solution:

100 mL	Glycerol, 99.5% (Carl Roth)
900 mL	RO-H_2O

Autoclaving was then carried out at standard conditions and followed by storage at 4 °C.

- 10x YNB (yeast nitrogen base):

35 g	Yeast Nitrogen Base (Amresco)
100 g	$(NH_4)_2SO_4$ (Sigma-Aldrich)
1000 mL	RO-H_2O

The solution was sterile filtered and stored at 4 °C

- 500x biotin stock solution:

4 mg	Biotin (Sigma-Aldrich)
20 mL	uHQ-H_2O

- 20 mM ABTS-solution:

396 mg	ABTS diammonium salt (Amresco)
36 mL	uHQ-H_2O

This solution was freshly prepared for every batch of BMG medium

- 10 mM $CuSO_4$-solution:

99.87 mg	Cu(II)$SO_4 \cdot H_2O$
40 mL	uHQ-H_2O

This solution was freshly prepared for every batch of BMG medium

- FBSM fermentation medium (Invtrogen):

26.7 mL	Phosphoric acid, 85 %
0.93 g	Calcium sulfate
18.2 g	Potassium sulfate
14.9 g	Magnesium sulfate
4.1 g	Potassium hydroxide
40.0 g	Glycerol, 99.5 %
1000 mL	RO-H_2O

Autoclaving was then carried out at standard conditions.

- Pichia trace metal salts PTM_1 (Invitrogen):

6.0 g L^{-1}	Copper (II) sulfate
0.08 g L^{-1}	Sodium iodide
3.0 g L^{-1}	Manganese sulfate
0.2 g L^{-1}	Sodium molybdate
0.02 g L^{-1}	Boric acid
0.5 g L^{-1}	Cobalt chloride
20 g L^{-1}	Zinc chloride
65 g L^{-1}	Ferrous sulfate
0.2 g L^{-1}	Biotin
5 mL L^{-1}	Sulfuric acid

The solution was resolved in RO-H_2O and sterile filtered before stored at 4 °C.

2.4. Buffers

- KPP buffer (KH_2PO_4/K_2HPO_4)

This buffer system comprising the potassium salts of hydrogen phosphate and di-hydrogen phosphate (both Carl Roth) was used for the preparation of media at different pH values. The salts were dissolved in uHQ-H_2O and stored at room temperature.

Table 4: Recipe for the preparation of 100 mM KPP-buffer at different pHs

pH	KH_2PO_4 [g L^{-1}]	K_2HPO_4 [g L^{-1}]
5.0	134.1	2.6
6.0	118.2	22.9
6.5	92.0	56.0
7.0	54.1	104.9

- Citrate buffer (sodium citrate/citric acid)

The citrate buffer was prepared at a concentration of 100 mM for the use in Bradford's protein assay of purified laccase variants and fermentation samples. A 0.1 M stock solution of citric acid was prepared by dissolving 21.0 g L^{-1} citric acid monohydrate ($C_6H_8O_7 \cdot H_2O$) in uHQ-H_2O. A O.1 M sodium citrate stock solution was prepared by dissolving 29.4 g L^{-1} trisodium citrate dihydrate ($Na_3C_6H_5O_7 \cdot 2H_2O$) in uHQ-$H_2O$. Both chemicals were purchased from Sigma-Aldrich. Buffers of desired pH were produced by mixing varying volumes of stock solutions. The stock solutions were to be stored at 4 °C, the working buffers were prepared freshly as often as needed.

- Tris Acetate-EDTA buffer (TEA-buffer)

A stock solution of 50x TAE was prepared by dissolving 242 g Tris base (Sigma-Aldrich) in 750 mL uHQ-H_2O. Subsequently, 57.1 mL acetic acid (Sigma-Aldrich) and 100 mL 0.5 M ETDA (pH 8.0) were carefully added before the final volume was adjusted to 1000 mL. This buffer was stored at room temperature.

- McIlvain buffer (citric acid/ Na_2HPO_4)

The buffer system by McIlvain (T. C. McIlvaine, 1921) contains a mix of 0.2 M Na_2HPO_4 and 0.1 M citric acid monohydrate (Sigma-Aldrich) or citric acid anhydrous (Sigma-Aldrich). Stock solutions of both compounds were volumetrically mixed to result in a buffer system of distinct pH values in a range of pH 2.5 to pH 7.5. This buffer was used for the colorimetric enzyme assays, storage of purified enzyme and electrochemical measurements. The buffer solution as well as the citric acid stock solution was stored at 4 °C and prepared newly as often as possible.

Table 5: Recipe for the preparation of 100 mL McIlvain buffer at different pHs

pH	Citric Acid	Na_2HPO_4
2.5	91.4 mL	8.6 ml
3.5	69.7 mL	30.3 mL
4.5	54.6 mL	45.4 mL
5.0	48.5 mL	51.5 mL
5.5	43.1 mL	56.9 mL
6.5	29.0 mL	71.0 mL
6.8	22.8 mL	77.2 mL
7.0	17.6 mL	82.4 mL
7.5	7.9 mL	92.1 mL

2.5. Assays

2.5.1. Colorimetric Laccase activity assays

The enzyme catalyzed oxidation of the substrates 2,2'-azino-bis(3-ethylbenzthiazoline-6-sulphonic acid) (ABTS) and 2,6-Dimethoxyphenol (2,6-DMP) served as the fundamental principle to evaluate enzymatic activity in a colorimetric assay.

The detection of laccase activity with the O_2 dependent oxidation of ABTS is often referred to as the standard assay for laccases. The enzyme is capable of oxidizing ABTS to its radical cation specie $ABTS^{\cdot+}$ resulting in a shift of the absorbance spectrum to an absorbance maximum of 420 nm and development of a green color. The absorption coefficient at 420 nm (ε_{420}) is 36.0 $mM^{-1}cm^{-1}$.

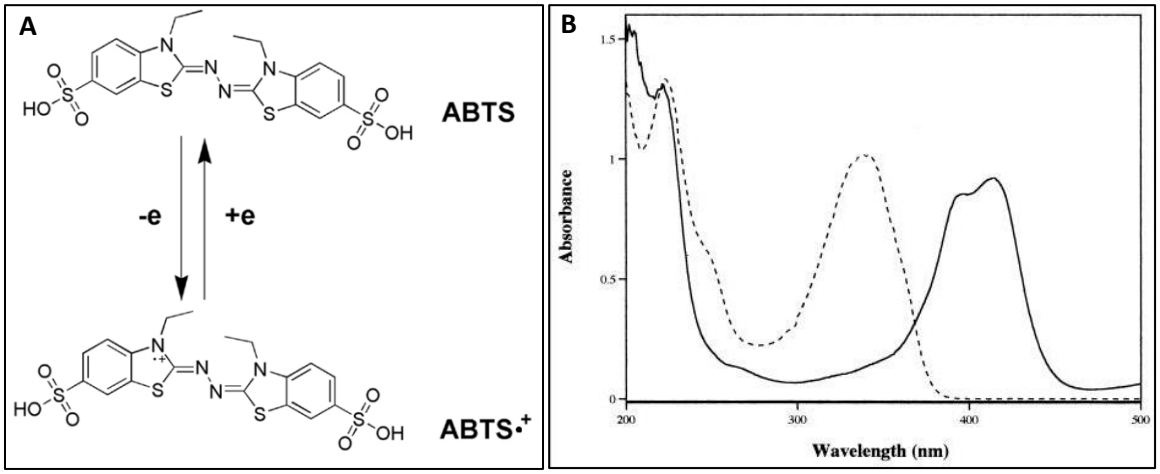

Figure 11: **A:** Oxidation of ABTS to its radical species (L. P. Christopher et al., 2014) **B:** The resulting spectrum shift of ABTS oxidation, dashed line (---) ABTS, solid line ABTS·+modified from Shi (Shi et al., 2011).

A second assay was used based on the oxidation of the phenolic substrate 2,6-DMP. The enzyme catalyzed reaction resulted in a shift in absorption maximum towards 469 nm and development of a deep amber color. The absorption coefficient at 489 nm (ε_{469}) is 49.6 $mM^{-1}cm^{-1}$.

Both chromogenic reactions allowed for simple use in a plate reader and a photometer set-up analysis. Furthermore, ABTS and 2,6-DMP solution were used in the protocols in an equivalent fashion, with the only exception being the different wavelengths measured (R. Kittl et al., 2012).

2.6. Molecular biology

2.7.1. Plasmid Isolation and Purification

The isolation of plasmids from transformed *E. coli* NEB 5-alpha was performed with the PureYield Plasmid Miniprep System (Promega). For the amplification of plasmids in *E. coli* culture, 3 mL of LB low salt Zeo$^+$ selection medium were inoculated with plasmid carrying cells in a lamina flow hood. Incubation was carried out overnight at 37 °C at a shaking speed of 125 rpm.
Plasmid isolation was performed according to Promega's alternative protocol for higher culture volumes with an Eppendorf 5424 centrifuge (Eppendorf AG, Hamburg, Germany). Elution was carried out with 20-50 µL nuclease free uHQ-H_2O. The flow through was retained in sterile Eppendorf tubes and stored at -20 °C.

2.7.2. Agarorse Gel Electrophoresis

A solution of 0.8 % *w/w* agarose (SERVA Electrophoresis GmbH, Heidelberg, Germany) in 1xTAE buffer was mixed with the suitable amount of 20000x peq-GREEN (peqlab, Erlangen, Germany) DNA dye in the gel tray and let cure for 30 minutes. The gel was then placed in the electrophoresis chamber and TAE buffer was added till the level of liquid exceeded the top of the gel slightly.
The DNA samples were arranged with 6x Loading Dye (Thermo Fisher Scientific), vortexed and applied to the pockets of the gel. GeneRuler DNA Ladder Mix (Thermo Fisher Scientific) was used alongside the samples as a DNA standard. Electrophoresis was performed at 100 V for 20-30 min on a PowerPac 300 (Bio-Rad Laboratories, Hercules, CA, USA) machine and results could be observed by using UV illumination in a GelDoc 2000 (Bio-Rad Laboratories) documentation system. If required, DNA bands of interest were excised from the gel with a scalpel and transferred into a sterile Eppendorf tube for further treatment.

2.7.3. DNA Gel Band Elution and Purification

DNA was eluted and purified from agarose gels by means of the Illustra GFX PCR DNA and Gel Band Purification Kit (GE Healthcare, Uppsala, Sweden). After pieces have been excised from the gel, their weight was determined and noted. The following steps of dissolving the agarose pieces, caption, centrifugation, washing and elution were performed in accordance to the manual's standard protocol for purification with reagents delivered by the supplier. Elution was to be carried out with 20-50 µL nuclease free uHQ-H_2O. The flow through was retained in sterile Eppendorf tubes and stored at -20 °C.

2.7.4. Error Prone PCR

For the creation of a mutational library of BaLac with error prone PCR (epPCR), a T383I I424M variant of the wild type gene was used as template. The gene was isolated and purified from an overnight culture of *E. coli* NEB 5-alpha (New England Biolabs), bearing the mutant gene in a BAGANSN vector construct. The plasmid solution was previously analyzed by spectroscopy at 260 and 280 nm in a DU 800 Photometer (Backman Coulter) to be sufficiently pure. The measurement of the plasmid solution revealed a DNA concentration of 331 µg mL^{-1}.

The error prone PCR was performed with a Gene Morph II Random Mutagenesis Kit (Agilent Technologies). The PCR protocol was tested with the guidance of the supplier's manual for a series of different concentrations of DNA template and varying numbers of PCR cycles to yield a desired mutation rate of five mutations per gene in the DNA sequence. The reaction was performed with 33.1 µg mL^{-1} template DNA.

Table 6: Recipe and PCR thermo-cycler program for the standard epPCR reaction with Gene Morph II Kit, 25 µL

	Substance in content	remarks	PCR thermo-cycler program		
2.5 µL	DNA Template	T383I I424M, BAGANSN	Denaturation	95 °C - 360 s	1x
2.5 µL	reaction buffer	10x Mutazyme II RB		95 °C – 30 s	19x
0.5 µL	dNTPs	10 mM each A,C,G,T			
0.5 µL	Forward primer	10 pg μL^{-1} pGAPfw2,	Annealing	56 °C – 30 s	
0.5 µL	Reverse primer	10 pg μL^{-1} 3ZLHGAP1rev			
0.5 µL	DNA Polymerase	Mutazyme II	Elongation	72 °C – 120 s	
18.0 µL	uHQ-H_2O	Nuclease free, sterile		72 °C – 420 s	1x

The stated program was used for the epPCR reaction in a C1000 Thermal Cycler (BioRad).

The obtained reaction mixes were then run on an agarose gel electrophoresis to separate the circular template plasmids (theorethical size of 4562 bp) from the amplified PCR product (1831 bp respectively). DNA Bands were purified from the gel, eluted in 26 µL nuclease free uHQ-H_2O and prepared for digestion with *Dpn*I to remove template plasmids from the solution.

2.7.5. *Dpn*I digestion

The endonuclease *Dpn*I is known to recognize methylation patterns of DNA and specifically cuts Gm6A^TC sites which are evident in DNA originating from *E.coli* replication. This feature particularly allows elimination of DNA template from PCR reactions which is necessary to exclude non-mutated plasmids from mutational libraries.

3 µL Tango-Buffer were added to 26 µL of purified PCR reaction product before 1 µL *Dpn*I restriction

enzyme was added to start the digestion. The reaction was performed at 37 °C for 60 minutes with gently shaking. The reaction was stopped by heat inactivation at 65 °C for 10 min. Buffer and enzyme were removed from the mix with Illustra GFX Purification Kit (GE Healthcare) protocol for DNA purification from enzymatic reactions.

2.7.6. Amplification PCR

To increase DNA content in order to elevate the transformation output, a second round of PCR was performed to pursue the epPCR. For this approach, 1:50 dilutions of the *Dpn*I-digested product were used as a DNA template in Go*Taq*-Polymerase G2 PCR reactions. Again, pGAPfw2 and 3ZLHGAP1rev were used to prime the replication. The experimental set-up for the reaction was as follows:

Table 7: Recipe and PCR thermo-cycler program for the amplification PCR with Go*Taq* G2 polymerase, 25 µL

	Substance in content	remarks	PCR thermo-cycler program		
1.0 µL	DNA Template (1:50)	BaLac T383I I424M	Denaturation	95 °C - 360 s	1x
5.0 µL	reaction buffer	5X Go*Taq* RB		95 °C – 30 s	35x
0.5 µL	dNTPs	10 mM each A,C,G,T			
1.0 µL	Forward primer	10 pg μL^{-1} pGAPfw2,	Annealing	60 °C – 30 s	
1.0 µL	Reverse primer	10 pg μL^{-1} 3ZLHGAP1rev			
0.5 µL	DNA Polymerase	Go*Taq* G2	Elongation	72 °C – 120 s	
16.0 µL	uHQ-H_2O	Nuclease free, sterile		72 °C – 600 s	1x

The PCR product was again applied to gel electrophoresis, excised from the gel, purified and eluted in 45 µL of uHQ-H_2O and stored at -20 °C.

2.7.7. Digestion and ligation

The purified PCR product was double digested with the restriction enzymes *Not*I and *Nde*I. 45 µL of PCR product solution were added to 1 µL of *Not*I, 1 µL of *Nde*I and 5 µL 10x Buffer O. The so obtained enzymatic mix was incubated at 37 °C overnight and run on a gel electrophoresis to separate the gene from the cut ends to be referred to as the insert. The digested product was purified from the gel prior to elution in 40 µl uHQ-H_2O.

In a similar approach, pGAPZA vector DNA was digested with *Not*I and *Nde*I to create a plasmid backbone for the ligation with the insert. After digestion, the solution was treated with FastAP to prevent undesired re-ligation and heat inactivated at 75 °C for 5 minutes to stop the reaction.

The ligation of backbone and insert was to be performed at an estimated ratio of 1:3. This proportion was determined via gel electrophoresis and UV illumination of small amounts of both solutions. A standardized thermal cycler program, comprising 16 consecutive 0.5 °C steps from 10 °C to 16 °C,

was performed for 60 minutes per step to ligate the samples. Samples were then automatically stored at 4 °C in the thermal cycler.

- Ligation reaction:

19 µL	Insert: *Not*I/*Nde*I digested PCR product
10 µL	Backbone: *Not*I/*Nde*I/ digested pGAPZA vector
3.5 µL	T4 Ligase buffer
2 µL	T4 Ligase

The ligation reaction was terminated by inactivation at 65 °C for 10 minutes. The purification of the ligated plasmids from the enzymatic mix was omitted and instead the inactivated mix was used directly for transformation in *E.coli* NEB 5-alpha cells.

2.7.8. High efficiency transformation of *E. coli* NEB 5-alpha

For the transformation of the previously created mutational library plasmids into chemo-competent *E.coli* NEB 5-alpha, the standard protocol for high efficiency transformation – "heat shock transformation" (New England Biolabs) was used. All steps were performed according to the user's manual with reagents and media delivered by the supplier.
200 µL of transformed cell suspension, pure or diluted, were plated on LB-ls agar plates with Zeocin or Ampicillin supplemented. For the creation of a mutational library on 200 mL LB-ls Zeo^+ agar plates, 1 mL cell suspension was streaked out.

2.7.9. Assessment of mutation rates

To ascertain that mutation rates for library creation remained in a desirable range of approximately five (DNA) mutations per gene, it was necessary to clone BaLac gene variants into a vector for sequencing. Alternatively to the approach of *Not*I/*Nde*I digestion and ligation the pJET cloning kit was used to for reasons of time saving.

Double digestion approach:

The amplified and purified PCR product was digested and ligated as described in 2.7.7. After transformation with the high transformation efficiency protocol, 200 µL of undiluted and 1:10 diluted cell suspension, respectively, were plated onto LB-ls Zeo^+ selection plates and incubated at 37 °C bottom up overnight. Isolated colonies were picked to inoculate 3 mL LB-ls Zeo^+ medium.

pJET approach:

In this approach, the amplified and purified PCR product was cloned into a pJET1.2/blunt cloning vector. The CloneJET PCR cloning kit (Thermo Fisher Scientific) comprises a blunting enzyme that is necessary to endow the PCR product, obtained by replication with a non-proof-reading polymerase, with blunt ends. The following steps of the cloning procedure were carried out according to the manual's standard Sticky-End Cloning Protocol with reagents provided by the supplier. 200 µL of diluted and 1:10 diluted cell suspension, respectively, were plated onto LB low salt Amp^+ medium and incubated at 37 °C bottom up overnight. Isolated colonies were picked to inoculate 3 mL LB-ls Amp^+ medium.

The inoculated cultures were grown overnight at 37 °C while shaking at 130 rpm. Plasmids were isolated and purified from the bacterial suspension as described in 2.7.1.Three aliquots of the eluted plasmid suspensions obtained by double digestion or pJET cloning were equipped with a set of appropriate primers for DNA sequencing.

2.7.10. DNA sequencing

To reveal alterations in the DNA sequence from the entire plasmid, it was necessary to cover the 5' priming end, the 3' priming end and the middle sequence of the mutational plasmids with suitable primers. The standard primers: pGAPfw2 (5' end), 3GAPZLH1rev (3'end) and 3BAL (middle) were used. To perform three sequencing reactions, three times 15 µL of purified plasmid solution, obtained as described above, were added 3 µL primer mix of a distinct type in an Eppendorf tube. Overnight sequencing was performed by Microsynth (Balgach, Switzerland) economy run service for plasmid DNA. Samples were analyzed in duplets. Sequencing results were compared to the BaLac-*wt* with the aid of the Clustal Omega alignment tool (EMBL European Bioinformatics Institute, Saffron Walden, UK)

2.7.11. Preparation of a cryo stock culture

To preserve cultures of mutational *E.coli* clones carrying genes of interest, an isolated colony was picked from an agar plate and used to inoculate 3 mL LB-ls medium for overnight incubation at 37 °C, 125 rpm. Alternatively, 500 µl of fresh library *E. coli* culture were used. Sterile 30 % glycerol was added to double the volume and 1 mL aliquots of this mix were transferred to cryo-tubes which were then stored at -80 °C.

This procedure was used in a similar fashion to conserve *P. pastoris* clones, with the exception of cultivation of desired clones being carried out in YPD at 30°C, 125 rpm.

2.7.12. Transformation of *P. pastoris* cells

Plasmid DNA isolated from *E. coli* cultivation with previously described methods was linearized in a *Pag*I digestion prior to the transformation into *P. pastoris* cells.
The described enzymatic mixture was incubated at 37 °C, shaking at 650 rpm for 240 min before reaction was stopped via heat treatment at 80 °C for 20 min. DNA was not purified from the enzymatic mix.

- *Pag*I digestion reaction:

30 µL	library plasmid solution
10 µL	uHQ-H_2O, nuclease free
4.5 µL	Buffer O
1.0 µL	*Pag*I

MicroPulser 1mm electroporation cuvettes (Bio-Rad Laboratories) were prepared for electroporation by washing with ethanol, drying at 50 °C and 10 min UV sanitation.
50 µl frozen *P. pastoris* X33 cells were thawed on ice until cell suspension was fully liquid. 4 µL of library plasmid solution were added to the suspension, gently stirred with a pipette tip and let stand for 10 minutes on ice. This mix was then transferred to the pre-chilled cuvettes by slow pipetting to the cuvette's wall to avoid bubble formation.
Subsequently, the cuvette was placed into the MicroPulser electroporation system (Bio-Rad Laboratories) and electroporation was performed with a voltage of 1.5 kV, 125 Ω during a 3.0 ms pulse. Swiftly, 500 µL ice cold sterile 1M sorbitol were added to the cuvette and briskly mixed by pipetting before 500 µL YPD were added. The suspension was then quantitatively transferred to a 2 mL Eppendorf tube and incubated horizontally shaken at 180 rpm for 3-4 hours.
1 mL of the transformed cell suspension was plated onto 200 mL YPD Zeo^+ Agar plates and incubated for 48 h at 30 °C.

2.7.13. Colony PCR

The isolation and amplification of genomic DNA from cultures of *P. pastoris* was approached with colony PCR. For this purpose, a small piece of cell material derived from a colony of overnight incubation was conveyed to 30 µL sterile uHQ-H_2O and boiled at 95 °C for 10 minutes to lyse the cells and free DNA. The cell debris was separated from DNA by centrifugation at maximum speed. 10 µL of the supernatant were used as a template for the following PCR reaction.

Table 8: Recipe and PCR thermo-cycler program for the colony PCR reaction with Go*Taq* G2, 25 µL

	Substance in content	remarks	PCR thermo-cycler program		
10.0 µL	DNA Template	Cell lysis supernatant	Denaturation	95 °C - 120 s	1x
5.0 µL	reaction buffer	5X Go*Taq* RB		95 °C – 30 s	34x
0.5 µL	dNTPs	10 mM each A,C,G,T			
1.0 µL	Forward primer	10 pg μL^{-1} pGAPfw2,	Annealing	60 °C – 60 s	
1.0 µL	Reverse primer	10 pg μL^{-1} 3AOX			
0.5 µL	DNA Polymerase	Go*Taq* G2	Elongation	72 °C – 120 s	
7.0 µL	uHQ-H_2O	Nuclease free, sterile		72 °C – 420 s	1x

The following program was used for the colony PCR reaction in a C1000 Thermal Cycler (Bio-Rad Laboratories). The PCR product was again applied to gel electrophoresis, excised from the gel and eluted in 45 µL uHQ-H_2O then stored at -20 °C. The so obtained samples were sequenced to reveal mutational changes in the gene sequence.

2.7.14. Creation of an mutational library via error prone PCR

The *B. aclada* laccase variant T383I I424M, a double mutant comprising the T383I mutation for higher thermal stability and the I424M mutation responsible for a shift in pH optimum, served as a template gene for a directed evolution approach. The gene template was available inserted in a BAGANSN vector, as a plasmid solution.

As described in 2.7.4, the gene was randomly mutated with error prone PCR at a mutation rate of 5 mutations per gene, as obtained from previous analysis 2.7.9. The PCR product was separated from the template via gel electrophoresis, purified and eluted in uHQ-H_2O. In the next step, *Dpn*I digestion was performed to remove non-mutated template DNA (2.7.5), the yielded DNA solution served as a template for the amplification PCR (2.7.6). Again, the reaction product was purified from the mix with gel electrophoresis and the purification kit. Consequently, the amplified DNA was double digested with *Not*I and *Nde*I, purified and ligated with a pGAPZA vector (2.7.7).

Twelve 9 µL aliquots of the ligated DNA were transformed into NEB 5-alpha cells as described in 2.7.8.LB-ls Zeo^+ plates were inoculated with 2 mL of transformed cell suspension each and incubated at 37 °C for 36 h. The cells were gently harvested from the agar plates with LB-ls Zeo^+ medium and a spatula, centrifuged at 4000 rpm for 5 minutes and re-suspended in 6 mL fresh media to be incubated at 37 °C, 130 rpm for 60 minutes. Furthermore, a 500 µL aliquot was gathered to be used to prepare a cryo stock for storage 2.7.11. Isolation of plasmid DNA from the *E.coli* library was carried out in ten parallel preparations according to 2.7.1 to yield 300 µL of purified library DNA which was subsequently digested with *Pag*I and transformed into *P. pastoris* like noted in 2.7.12.

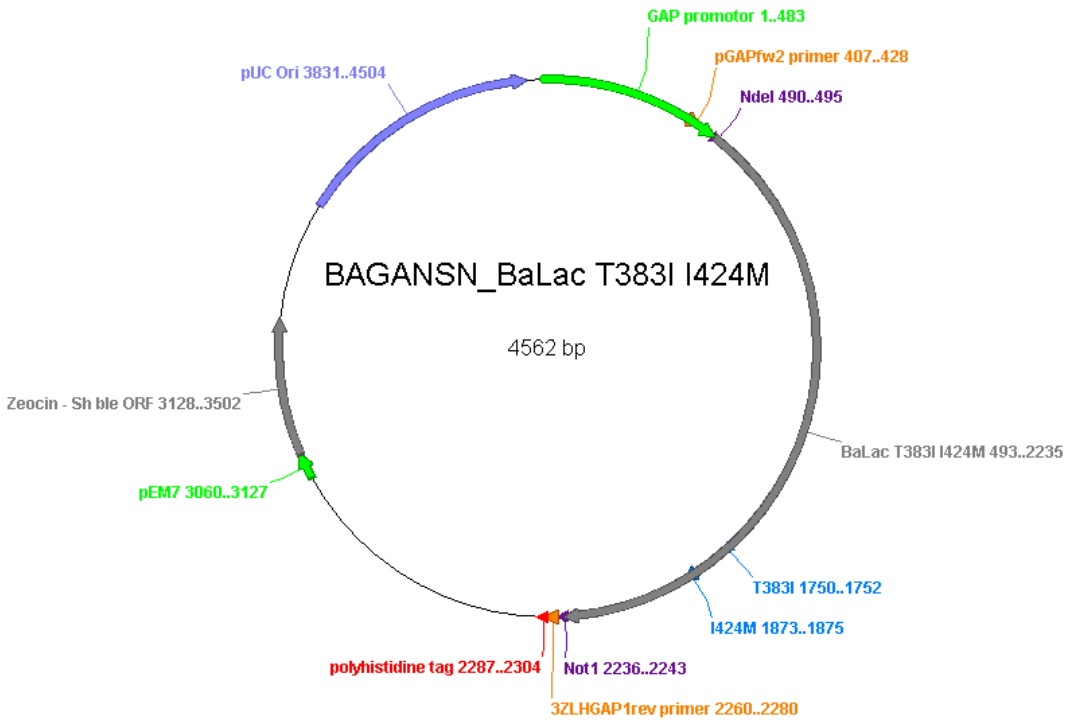

Figure 12: Vector map of the BaLac T383I I424M variant cloned in a modified pGAPZA backbone (BAGANSN). The different features are marked in the various colors and stated with the positions in the vector.

Table 9: List of vector features and their positions in the vector map

Name	Type	Location
T383I	variation	1750..1752
I424M	variation	1873..1875
*Nde*I	restriction site	490..495
*Not*I	Restriction site	2236..2243
pGAPfw2 primer	primer_bind	407..428
3ZLHGAP1rev primer	primer_bind	2260..2280
BaLac T383I I424M	gene	493..2235
polyhistidine tag	purification tag	2287..2304
GAP promoter	promoter	1..483
pEM7 promoter	promoter	3060..3127
Zeocin - Sh *ble* ORF	gene	3128..3502
pUC Ori	rep_origin	3831..4504

2.8. High throughput screening

The process of variant screening shall be separated into two major steps: the pre-screening and the differential screening, last of both, embracing two different methods for the analysis of pH and stability characteristics of the enzyme.

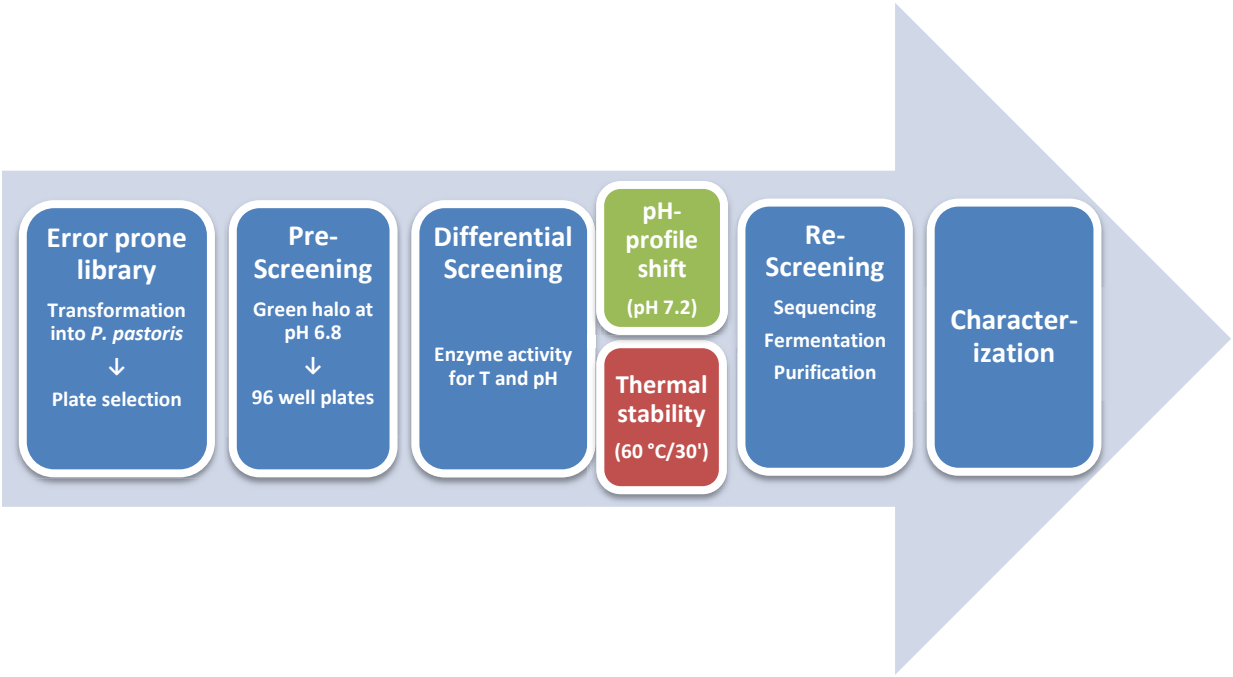

2.8.1. Pre-screening

Incubated 200 mL YPD Zeo$^+$ plates, obtained from electroporation of *P. pastoris* X33 cells with library DNA were to bear circa 500 to 1000 colonies. These colonies were duplicated onto selective BMG pH 6.5 Agar plates with assistance of a sterile cotton sheet. By pressing the incubated YPD plate gently onto a sheet draped over a flat and sterile surface, little cell material was collected from the colonies and distributed in the same pattern onto a BMG plate. The plates were then incubated at 30 °C for 48 to 72 hours. After incubation, colonies expressing functional variants of the *B. aclada* laccase presented green halos deriving from enzymatic conversion of the contained ABTS. Those, regarded positive, clones were gathered in patterns resembling 96 well plates on fresh YPD Zeo$^+$ plates by means of picking with sterile toothpicks or the use of an automated picking robot program.

2.8.2. Differential screening

The wells of sterile 96 well microtiter plates (Greiner, Kremsmünster, Austria) were filled with 210 µL BYPD (200 mM KPP, pH 5.0) medium and inoculated with selected colonies from the previous pre-screening. Five duplicates of a clone expressing the parental BaLac T383I I424M were added to reserved spaces on the plate to allow for comparison in the screening process. Sealing was then obtained via Breathe Easy membranes (Sigma-Aldrich) to avoid reduction of the culture volume by

means of evaporation. Incubation was carried out at 30 °C, 320 rpm shaking and 90 % relative humidity for 48 hours.

When incubation was completed, cell material was separated from the supernatant by centrifugation at 3000 rpm for 10 min with a 5804 swing bucket centrifuge (Eppendorf). With the use of a JANUS automated workstation (PerkinElmer, Waltham, MA, USA) 100 µL culture supernatant were collected from each well and distributed as 20 µL aliquots into fresh 96 well plates. Each well were then added 100 µL McIlvain Buffer of desired pH and 80 µL 2.5 mM ABTS or 2,6-DMP substrate solution subsequently. Measurement was then performed in an EnSpire Multimode plate reader (PerkinElmer) and carried out over a period of 180 seconds. For ABTS and 2,6-DMP, detection wavelengths of 420 nm and 469 respectively were used. Ten reading points were to document the OD at given time and resulted in a kinetic curve, characteristic for the enzymatic activity of a variant.

Alterations in the performance of specific variants could be assessed with photometric assays as described. Two distinct features of the enzymatic variants were of interest:

- Activity at increased pH: The assay was performed with the enzyme solution being exposed to buffer of pH 5.0 and pH 6.8. It was carried out in parallel with ABTS and 2,6-DMP as substrates . The output was stated as relative conversion activity at pH 6.8 with respect to that at pH 5.0 for both substrates.
- Thermal stability: This assay was performed solely with ABTS at pH 5.0. Incubation was carried out at 60 °C for 30 min. The conversion of ABTS at pH 5.0 after incubation was related to the ABTS conversion at pH 5.0 of untreated sample.

To sum up, five assays were used to evaluate a clone's performance in the differential screening:

Table 10: Assay matrix for assessment of variant performances in directed evolution

Assay	Substrate	wavelength	pH	Strategy
Activity	ABTS	420 nm	5.0 | 6.8	Relative activity (activity at pH 6.8 vs. activity at pH 5.0) compared to relative activity of parental enzyme
	2,6-DMP	469 nm	5.0 | 6.8	
Thermal stability	ABTS	420 nm	5.0	Relative activity at pH 5.0 as incubated vs. non-incubated sample compared to parental enzyme

As mentioned before, relative activities of catalytic conversion at various testing conditions were obtained by comparison to activity at pH 5.0. In data processing, this was applied according to the following formula:

$$Relative\ activity = \frac{Activity\ at\ testing\ condition}{Activity\ at\ pH\ 5.0}$$

In a further step, those obtained relative activities were compared to the mean relative activity of five parental clones. To be considered an improved variant, a colony needed to exceed the average parental performance by at least three fold its standard deviation. In a consecutive evaluation procedure, the quality of data was examined by means of the R^2 of the kinetic slopes. A minimum of $R^2 = 0.7$ was required for a measurement to remain in the data set before visual control was to support the result.

2.8.3. Re-screening

Colonies which showed an improved activity in the differential screening were gathered for a re-screening and were plated again alongside parental clones on a fresh YPD Zeo^+ agar plate. To minimize positional and operational bias, clones were prepared as quadruplets, equally distributed over the 96 well shaped pattern of the plate. A copy of this plate was prepared to be measured in a second repeat in reverse order.

Incubation was then carried out under standard conditions for yeast: 30 °C, 48 h. Agar cultivation was again followed by inoculation in 210 µL BYPD medium in sterile 96 well plates and cultivation at 30 °C, 320 rpm shaking and 90 % relative humidity for 48 hours. Activity assessment of the clones was performed identical to the prior procedure with one exception: to reveal information about the levels of expression, kinetic slopes of ABTS conversion at pH 5 were compared to the parental clone as well. Thus, pH dependent 2,6-DMP conversion (2,6-DMP $pH_{6.8}/pH_{5.0}$), pH dependent ABTS conversion (ABTS $pH_{6.8}/pH_{5.0}$), thermal treatment dependent ABTS conversion (ABTS T_{60}/T_{RT}) and expression levels were parameters to assess most the promising variants. Again, R^2 values smaller than $R^2 = 0.7$ were released from the data processing.

If former results could be confirmed, isolated colonies were picked on fresh YPD Zeo^+ plates, streaked out and incubated overnight at 30 °C. Colony PCR was used to isolate and amplify genomic DNA from desired colonies before sequence variations in the BaLac gene were analyzed via DNA sequencing.

2.9. Fermentation & purification

The recombinant production of *Botrytis aclada* laccase variants in *P. pastoris* was performed in a 0.5 L scale Multifors fermenter system (Infors HT, Bottmingen, Switzerland) and was carried out on the basis of the "Pichia Fermentation Process Guidelines" by Invitrogen. A fed batch feeding strategy was selected to control the process. Samples were drawn periodically to allow monitoring of wet biomass, total soluble protein content and laccase activity. In a primary capture procedure, the fermentation broth was harvested and supernatant was refined by centrifugation before a combination of ammonium sulfate precipitation and centrifugation was performed to increase product purity.

A two-step chromatography purification operation was used and was equipped with phenyl based columns for hydrophobic interaction separation. Desired fractions were united, enriched by filtration and stored at -80 °C. (R. Kittl et al., 2012)

2.9.1. Batch phase

20 mL pre-cultures of desired clones (YPD medium in shaking flask, incubation: 48 h, 25 °C, 250 rpm) were used to inoculate 0.4 L sterile FBSM medium supplemented with 0.1 mM copper (II) sulfate and anti-foam. During the batch phase, constant process parameters were to be maintained at 1000 rpm stirring and 2 L min^{-1} aeration with air. For pH regulation, NH_4OH supply was used to preserve a pH of 5.5. The fermentation was performed at 25 °C.

2.9.2. Feed phase

After substrate limitation, representing the end of the batch phase, was observed, a constant feed of 2.0 mL min^{-1} was started. The feed medium contained 50 % (w/w) glycerol supplemented with 12 mL L^{-1} PTM_1 salt solution. Furthermore, aeration was adapted to be carried out with 0.5 L min^{-1} oxygen. The feed rate was manually adjusted to sustain oxygen saturation (cO_2) of at least 20 %.

2.9.3. Primary capture

Circa 500 mL of fermentation broth were gathered in 250 mL volumes and centrifuged at 6000 g and 4 °C for 30 min in a Optima L-70 Ultracentrifuge (Beckman Coulter, Pasadena, CA, USA) Subsequently, $(NH_4)_2SO_4$ was added to a final concentration of 40 % to precipitate unspecific byproduct. The precipitate was separated via overnight sedimentation in the 4 °C cold room and the supernatant was gently transferred to fresh vessels in the next step to yield circa 320 mL crude extract.

2.9.4. Hydrophobic interaction chromatography (HIC)

Purification of laccase was achieved by a combinatorial HIC procedure using an ÄKTA purifier and an ÄKTA explorer chromatography unit (GE Healthcare). The purification protocol embraced a 50 mM sodium citrate buffer pH 5.5, complemented with 40 % $(NH_4)_2SO_4$ for washing and loading (Buffer A) and a 50 mM sodium citrate buffer pH 5.5 without additional salt (Buffer B) for gradient elution. Prior to loading, conductivity of Buffer A and extract sample were balanced according to each other. Elution at a linear gradient from 40 % to 0 % salt saturation was supported by detection at 280 nm and 610 nm (R. Kittl et al., 2012).

- In a preliminary step, a 70 mL Penyl sepharose column (GE Healthcare) was loaded with crude extract. A washing step was performed with at least ten column volumes (CVs) of Buffer A before gradient elution was carried out in 96 7.5 mL fractions. Active fractions were examined for laccase activity with the plate reader assay (2.8.2.) and desired fractions were pooled.

- In a subsequent step of crossflow enrichment in a Fivaflow 50R device (10 kDa mwco, 50 cm², Sartorius, Germany) the volume from pooled fractions was reduced from 200 mL to 40 mL.

- Consecutively, a 20 mL Phenyl source column (GE Healthcare) was to formulate the final laccase solution. Laccase extract was loaded, washed with five CVs and eluted in 96 2.0 mL fractions. Obtained samples were again tested for activity, pooled and then concentrated in a filtration approach with Amicon Ultra-15 Centrifugal Filter Units (30 kDa mwco, 7.6 cm², Millipore, USA). During filtration, chromatography buffer was exchanged for McIlvain buffer pH 4.5.

2.9.5. SDS PAGE

Samples of purified BaLac variants were assessed for concentration as described in (2.10.2.) and diluted to 0.15 mg mL^{-1} with McIlvain buffer pH 4.5. They were then mixed with Laemmli-buffer (Thermo Fisher Scientific) and denatured at 95 °C for 5 min. 13 µL sample were loaded on a Mini Protean Precast Polyacrylamid Gel (Bio-Rad) accompanied by 10 µL of Precision Plus Protein Unstained Standard, (Bio-Rad). Band separation was run for 60 min at 120 V. Staining was accomplished with Bio-Rad staining solution.

2.10. Characterization

To keep record of progress and efficiency of the fermentation and purification protocol, samples were drawn from all major steps to state information about wet cell mass, protein concentration, and volumetric activity. Specific enzyme activity was calculated from volumetric activity and protein concentration.

2.10.1. Wet biomass

1 mL fermentation samples were drawn in Eppendorf tubes and centrifuged at maximum speed for 5 minutes. Supernatant was removed from the tube and the pellet was weighed to reveal wet biomass in units of mg mL^{-1}.

2.10.2. Protein concentration

The method for determination of protein concentration by Bradford (M.M. Bradford, 1976) was used for evaluation of laccase concentrations from fermentation fractions. Homogeneous samples, obtained from chromatographic separation, were analyzed by means of photometrical measurement at 280 nm.

2.10.3. Bradford protein assay

In this approach, cuvettes were filled with 600 µL Bradford reagent before 15 µL of enzyme solution were added. Samples were incubated for 15 minutes and photometric measurement was executed with a DU-800 Photometer (Beckman Coulter, USA).
Calculation of protein concentrations were carried out with respect to a 0.1 - 1.0 mg mL^{-1} series of BSA dilutions in 0.15 M NaCl, 0.05 % NaN_3 (Protein Standard Sigma P-0914). Measurements of purified enzyme samples were designed as duplicates to cover a range of 1:10 to 1:10000 dilutions in 100 mM citrate buffer pH 5.0.

2.10.4. Spectrophotometrical measurement

The absorption spectra of homogeneous laccase solution from 230 nm to 800 nm were determined in 0.3 mm quartz cuvettes in a Hitachi U-3000 spectrophotometer (Hitachi, Tokyo, Japan) with a scan rate of 60 nm min^{-1}. The obtained absorption at 280 nm, the absorption coefficient ε_{280} = 125 290 M^{-1} and the approximated molecular weight of *Botrytis aclada* laccase of 61 565 g mol^{-1} yielded the concentrations of homogeneous samples.

2.10.5. Volumetric activity

The standard assay for laccase activity with ABTS served to determine volumetric activities from both fermentation samples and purified laccase solution.

The measurements were performed with a Lambda 35 UV/VIS spectrophotometer (PerkinElmer). Enzyme samples were prepared in proper dilution with 100 mM citrate buffer pH 4.0. 100 µL 10 mM ABTS solution, 880 µL 100 mM citrate buffer pH 4.0 and 20 µL sample were mixed in cuvettes and incubated at 30 °C for 10 minutes. Kinetic curves were recorded during 180 s of analysis. The volumetric laccase activity, stated in units per mL, was calculated from the acquired kinetic slopes by multiplication with the enzyme factor (EF).

One unit of activity was defined as the amount of enzyme required to obtain 1 µmol of product per minute. (E. Osipov et al., 2014)

$$\frac{cuvette volume\,[\mu L] \times sample\ dilution\ \ factor}{sample\ volume\,[\mu L] \times \varepsilon} = enzyme\ \ factor(EF)$$

2.11. Electrochemical assessment

Electrochemical investigations on various BaLac variants were performed at the Department of Biomedical Science at Malmö University, Sweden.

2.11.1. Chemicals

All chemicals used were of highest purity available.

Citric acid monohydrate $C_6H_8O_7 \cdot H_2O$, (Sigma-Aldrich)

Disodium phosphate dehydrate $Na_2HPO_4 \cdot 2H_2O$ (Sigma-Aldrich)

Potassium molybdocyanide $K_4[Mo(CN)_8]$ (Sigma-Aldrich)

Potassium ferrocyanide $K_4[Fe(CN)_6]$ (Merck)

Potassium tungstocyanide $K_4[W(CN)_8]$, home synthesized

37 % Hydrogen peroxide H_2O_2 (Merck)

96 % Sulfuric acid H_2SO_4 (Merck)

Multi walled carbon nanotubes (o.d. 10-15 nm, i.d. 2-6 nm, l. 0.1 – 10 µm) (Sigma-Aldrich)

All solutions were prepared using deionized water (18 MΩ·cm) from a PURE-LAB UHQ II system by ELGA VEOLIA (Lüneburg, Germany).

2.11.2. Enzymes

The enzymes were stored at -18°C in aliquots of 5 to 50 µl until further use.

2.11.3. Investigations of midpoint potential - cyclic voltammetry (CV)

Cyclic voltammograms (CVs) of the various *Botrytis aclada* laccase variants were recorded initially to identify possible outliers in midpoint potentials (E_m) in order to obtain a universally eligible setup for further electrochemical investigations.

- Electrode preparation:

Glassy carbon electrodes (GCEs) with a geometric carbon surface area of 0.071 cm^2 were purchased from BASi (BAS, West Lafayette, IN USA). These planar electrodes were mechanically cleaned through polishing on Microcloth paper (Buehler, Coventry, UK) with an aluminum oxide suspension of 0.1 µm particle size (Struers, Ballerup, Denmark). To remove residual aluminum oxide the GCEs were rinsed with deionized water and sonicated for 5 min in an Ultrasonic Cleaner XB2 bath (VWR International Ltd., Lutterworth, UK). Prior to drying in an airflow the GCEs were again rinsed with deionized water. 4.5 mg of mwCNTs were suspended in 1.5 mL deionized water, vortexed and sonicated for 10 minutes to obtain a homogeneous suspension. 5 µL of this suspension were carefully pipetted onto

the GCE surface to form a steady drop and let dry for 15 minutes in a laminar flow hood. This procedure was repeated two more times to yield a nanocomposite coating of 640 µg cm^{-2}. The surface was then optically examined for a well-developed and sufficiently homogeneous distribution of the coating before proceeding with the measurement.

- CV measurements:

Cyclic voltammetry measurements were carried out using a µAutolab Type III/FRA2 potentiostat/galvanostat with GPES software (Metrohm Autolab BV, Schiedam, Netherlands). It was endowed with a three-electrode circuit comprising a saturated calomel electrode (SCE, $Hg|Hg_2Cl_2|KCl_{sat}$; 244 mV vs. normal hydrogen electrode NHE) serving as a reference electrode and a platinum wire as an auxiliary electrode. The measurement cell was set up with 50 mL of McIlvain buffer pH 4.5. All potentials are stated with respect to NHE, unless reported otherwise.
CVs (from +800 mV to 0 mV and back to +800 mV) were performed in two cycles under aerobic conditions (air) with a scan rate of 10 mV s^{-1}. Firstly, the measurement was carried out against buffer twice to clean the surface from potential electroactive impurities and to obtain a blank signal. After a swift immersion in deionized water and a subsequent drying in the laminar flow hood, 5 µL of freshly thawed enzyme solution were applied - without respect to the concentration - to the mwCNT modified GCE surface and enzyme immobilization was performed for 20 minutes. In this period, the electrode's surface was protected via capping with an eppendorf tube. In the next step an excess of enzyme on the surface was removed by immersion into buffer before the CV was recorded with the parameters similar to those of the blank measurement.

2.11.4. Investigations of pH dependence of E_m – cyclic voltammetry (CV)

To allow observation of the pH related change in E_m-values over a fairly broad pH range a series of McIlvain buffers of different pHs (2.5, 3.5, 4.5, 5.5, 6.5, 7.0 and 7.5) were prepared.
In comparison to the experimental procedure used for the investigations in midpoint potential, the cyclic voltammetry set up was performed with some changes in the measurement routine. To guarantee that the voltammograms obtained, presented the well-pronounced and uninfluenced redox transmission of the copper centers, it was necessary to perform all measurements in anaerobic environment. For this reason, all buffers were deoxygenated by flushing with Argon gas (AGA Gas AB, Lidingö, Sweden) for 15 minutes prior to blank and laccase measurement. Furthermore, argon gas was also flushed into the cell's head space during the actual measurements with respect not to disturb the covering on the electrode. In addition to that, the number of CV cycles was reduced from two to one in order to decrease exposure times of sample in unfavorable environment and to

guarantee proper redox transmission peaks. Again, all potentials are stated with respect to NHE, unless reported otherwise.

2.11.5. Spectroelectrochemical studies

A mediated spectroelectrochemical redox titration (MRT) procedure was used to determine the T1 site midpoint redox potentials (E_m) of *Botrytis aclada* laccase variants at pH 4.5. Direct spectroelectrochemical redox titration (DRT) was performed as well to study mediatorless electron transfer.

- Preparation of the spectroelectrochemical cell:

For the following experiments, a spectroelectrochemical cell, built and described by Andreas Christenson was used (A. Christenson et al., 2006).
To enhance the electron transfer between solute enzyme and gold electrode for the MRT experiments, 200 µM of the reduced forms of the redox mediators $K_4[Fe(CN)_6]$, $K_4[Mo(CN)_8]$ and $K_4[W(CN)_8]$ were used. This was necessary to minimize the influence of hysteresis and to cope with poor electronic contact and protein insulation on the bare gold electrode to obtain well-pronounced titration curves. The mediator mix is designed to cover a sufficiently large range of redox transition from approximately 400 mV to 800 mV. 100 µl aliquots of the various laccase variant enzyme solutions were prepared by diluting the stored samples with 0.2 M McIlvain buffer (pH 4.5) and the suitable amount of mediator mix to result in a final concentration of 3 mg mL^{-1} enzyme solution. One should be aware that the mediator solution, containing $K_4[W(CN)_8]$, should be protected from direct light to avoid photodecomposition and better be prepared just prior to its use. The enzyme sample was then aspirated trough the gold capillary (A. Christenson et al., 2006).

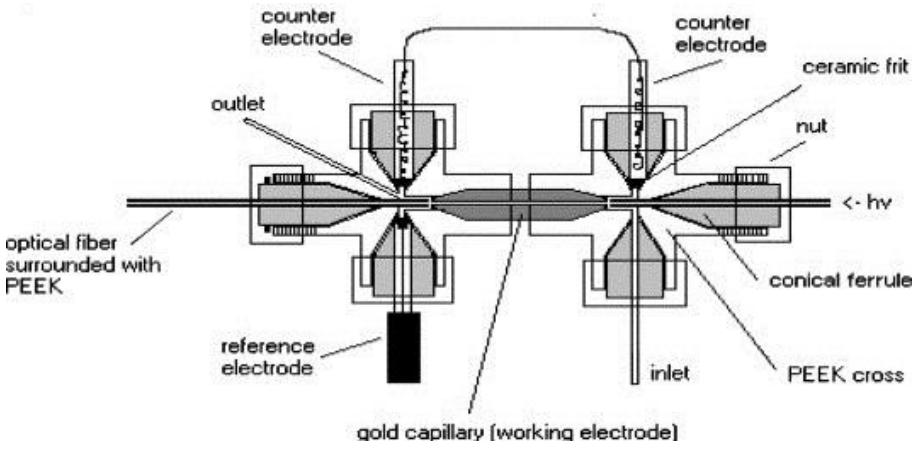

Figure 13: Scheme of the measurement cell (N. Bistolas et al., 2004). In this spectroelectrochemical setup, incenting light passes through the gold capillary interacts with the sample before being transmitted via fiber optics and being detected at the spectrometer. The sample can be influenced with an Ag|AgCl reference electrode and a platinum counter electrode in a three-electrode-setup.

- Redoxtitration measurement:

To attain midpoint potentials at pH 4.5 ($E_{m;4.5}$), a series of potentials was sequentially applied to the system to span a range of 1100 mV to 200 mV with 50 mV intervals. To guarantee Nernst equilibrium between the oxidized (Ox) and reduced (Red) form of the mediators, the current redox state of the enzyme and the electrode, it was necessary to maintain the distinct potentials applied for precisely 5 min each. This consecutive change of the redox state of the mediators resulted, in return, in a stepwise change of concentration of the reduced (Red) and oxidized (Ox) species of the laccase enzymes. Spectra were recorded for all individual equilibriums to represent the state of the [Ox]-to-[Red]-ratio at a certain potential applied. Basic titration parameters, such as $E_{m;4.5}$, b (slope of the titration curve), n (number of electrons) and r (correlation coefficient) were determined from plots derived from the Nernst equation. The fundamental principles and assumptions for the determination of oxidation and reduction potentials that form the basis for the electrochemical experiments of this work were described by G. S. Wilson and P. L. Dutton (P. L. Dutton, 1978; G. S. Wilson, 1978).

The experimental set up for DRT was identical to that of MRT with the exception that no mediators were added to the enzyme sample. All reported potentials are referred to NHE unless stated otherwise.

Data processing for all electrochemical calculations was performed with Origin Pro 8.6 (OriginLab, Northampton, MA, USA)

3. Results and Discussion

For reasons of structuration, the data and results obtained are presented in subcategories:

- Directed evolution
- Fermentation and purification
- Electrochemical investigation

Throughout this master thesis, different variants of *Botrytis aclada* laccase were used although the directed evolution approach was rooted solely by the BaLac T383I I424M clone. Comparison and collaboration made it necessary to include other variants than the ones obtained from directed evolution into fermentation and purification as well as into electrochemical investigation.
Table 11 gives an overview on the BaLac variants used during work.

Table 11: List of BaLac variants used for various approaches and investigations

Experiment	BaLac variant	Origin
Directed evolution	T383I I424M	Discovered by E. Breslmayr in 2014
Fermentation & purification	T383I	Discovered by S. Scheiblbrandner in 2013
	T383I I424M	Discovered by E. Breslmayr in 2014
Electrochemical investigation	Wild type*	Produced by Roman Kittl in 2013
	T383I*	Produced in the course of this work
	T383I I424M*	Produced in the course of this work
	T383I A180D	Produced by E. Breslmayr in 2014
	T383I I491N	Produced by E. Breslmayr in 2014
	I424S	Produced by E. Breslmayr in 2014
	I424G	Produced by E. Breslmayr in 2014
	D236E	Produced by E. Breslmayr in 2014
	S359F	Produced by Roman Kittl in 2013
	I491F	Produced by Roman Kittl in 2013
	L499F	Produced by Roman Kittl in 2013

* samples for electrochemical measurement were present in more than one fermentation batch

3.1. Directed evolution

In a first round of directed evolution with the wild-type BaLac gene, the exchange of a threonine (T) for an isoleucine (I) at position 383 (referred to as T383I) resulted in increased thermal stability, becoming manifest in increased melting temperature (T_m) and elevated half-life (T_{50}) particularly. The introduction of a second mutation to the T383I variant, namely the exchange of an isoleucine (I) for a methionine (M) at position 424 (referred to as I424M) had beneficial influence on the pH profile but was compromising the thermal stability (E. Breslmayr, 2015, unpublished).

3.1.1. Assessment of mutation rates for epPCR

Error prone PCR was performed with 83 ng BAGANSN_BaLac T383I I424M template DNA and 19 cycles of annealing, polymerization and denaturation as stated in 2.7.4. After amplification PCR and cloning, the DNA sequencing revealed five mutations per gene (see table 11). Two cloning approaches, the pJET cloning and the standard *Not*I/*Nde*I double digestion approach lead to the same result. In both cases, *Not*I and *Nde*I restriction sites were present. Both parental mutations were evident as well.

Table 11: Overview on assessment of mutation rates, positions and type of mutation

Feature	*Not*I/*Nde*I approach	pJET approach
*Nde*I restriction site (CATATG)	✓	✓
*Not*I restriction site (GCGGCCGC)	✓	✓
T383I: N1259 ACT → ATT	✓	✓
I424M: N1383 ATT → ATG	✓	✓
1st mutation	N66 TCC → ACC	N390 ACT → ACC
2nd mutation	N126 AGC → AAC	N1179 ACA → TCA
3rd mutation	N906 ACT → AAT	N1392 TAT → TGT
4th mutation	N1089 GCC → GTC	N1416 CTT → TTT
5th mutation	N1389 CAT → CAA	N1551 TAA → CAA

Notes: "✓" indicated the respective sequences were evident in mutational variants

3.1.2. Creation of a mutational library

To guarantee that theoretically all positions in the laccase gene are potentially mutated in a library, a library size of 50 000 variants was discussed to be sufficient. High efficiency transformation of mutational variants into competent *E. coli* NEB 5-alpha cells was performed until a library size of 50400 clones on selective Agar plates was reached. The subsequent isolation of plasmids from bacterial culture, electroporation into *P. pastoris* X33 cells and pre-screening plates resulted in circa

15 100 colonies expressing functional laccase. In a test, the efficiency of transformation for actively producing clones was reported to be approximately 30 % after 48 h of incubation on ABTS containing BMG Agar.

3.1.3. High throughput screening

A total of 3330 functional BaLac clones were assessed in 37 screenings during the differential screening phase. From each screening, the best clone to outperform the parental enzyme in terms of thermal stability was nominated for a re-screening. In addition to that, nine clones with shifted pH profile, in regards of ABTS or 2,6-DMP bio-catalysis, were selected as well. To sum up, 46 clones were to be further analyzed in a consecutive re-screening.

From the re-screening nine clones were confirmed to have increased activity after thermal treatment. One clone was confirmed to outperform the parental relative activity of ABTS catalysis. Sequencing was then carried out for all ten clones and revealed the following genetic content (Table 13): Eight clones, reported to have desirable stability properties were identified as T383I BaLac variants. Clone 1A9, proven to have improved ABTS bio-catalysis was identified as parental clone T383I I424M.

Table 12: Summary of re-screening results of ten high-performing BaLac clones stated as relative activities with standard deviation. n = 4 for the calculation of standard deviations.

Variant	Alias	ABTS T_{60}/T_{RT}	ABTS $pH_{6.8}/pH_{5.0}$	2,6-DMP $pH_{6.8}/pH_{5.0}$	Expression
parent	-	*1.00 ± 0.07*	*1.00 ± 0.32*	*1.00 ± 0.05*	*1.00 ± 0.15*
T383I	1A7	1.52 ± 0.08	1.12 ± 0.14	0.88 ± 0.18	1.96 ± 0.16
T383I	1A8	1.59 ± 0.01	0.81 ± 0.09	0.85 ± 0.09	1.27 ± 0.14
T383I I424M	1A9	1.08 ± 0.06	1.54 ± 0.10	1.02 ± 0.06	1.36 ± 0.12
T383I	1D5	1.56 ± 0.07	1.10 ± 0.08	0.77 ± 0.07	1.96 ± 0.18
T383I	1B6	1.56 ± 0.07	1.04 ± 0.11	0.77 ± 0.13	2.00 ± 0.07
T383I	1B10	1.53 ± 0.05	0.93 ± 0.11	0.74 ± 0.06	1.65 ± 0.12
T383I	2A6	1.33 ± 0.04	0.74 ± 0.10	0.73 ± 0.09	1.83 ± 0.05
T383I	2B5	1.39 ± 0.06	0.67 ± 0.10	0.69 ± 0.12	1.84 ± 0.09
T383I	2B6	1.35 ± 0.08	0.72 ± 0.13	0.78 ± 0.19	1.65 ± 0.19

3.1.4. Discussion

It could be shown that a mutation rate of 5 mutations per gene could be reached. Furthermore, sequencing was able to show that error prone was unbiased regarding nucleotide exchange.

The proportion of functional laccase in *P. pastoris* after transformation, stated with 30 % can be regarded as reasonable when considering the relatively high rate of mutations and the challenging cultivation conditions for the pre-screening at pH 6.5.

Relatively large standard deviations of the ABTS $pH_{6.8}/pH_{5.0}$ screening experiment indicated restricted accuracy. Comparison to the parental variant T383I I424M was only possible with greatest caution. The reason for this may root in the limited activity of catalytic activity at pH 6.8.

The issue of the detection of false-positive T383I I424M (1A9) clone as an improved pH variant may root as well in the large margin of error of the screening assay. Furthermore, different expression levels of the parental reference and the 1A9 clone might also have contributed to the miss-assessment.

The identification of eight BaLac T383I clones as improved variants is comprehensible since the addition of the I424M mutation compromised the thermal stability. Removing the I424G mutation should lead to increased performance in the thermo-stability screening. One should be aware that the various T383I clones all bear identical gene sequences, similar to the T383I ancestor (N1259 ACT → ATT). This is equally true for the T383I I424M (1A9) gene, which is a copy of the parental gene (N1259 ACT → ATT; N1383 ATT → ATG).

It is therefore unlikely that those variants origin from error prone PCR. A potential source might be an *E. coli* colony carrying the T383I plasmid from a former directed evolution transformation which contaminated a large LB Zeo^+ plate. Furthermore, the plasmid could also origin from a contamination in one of the components of the PCR reactions. The presence of a parental T383I I424M variant could be owed to an insufficient *Dpn*I digestion prior to the *E. coli* transformation.

Interestingly, the screening method was potent enough to enrich the T383I plasmid contamination several times during the course of the screening. Furthermore, since the impairing effect of the I424M on the thermal stability is relatively high, it could easily been possible that beneficial mutations were superimposed by the loss of the I424M mutation. In any case, the prominent screening principle: “You get what you screen for” by F. H. Arnold and A. A. Volkov (1999) again proved to be true.

3.2. Fermentation and purification

The use for biochemical characterization and electrochemical studies made it necessary to produce sufficient amounts of highly pure enzyme. It was decided to produce the two T383I clones 1A7 and 2A6 alongside the T383I I424M clone 1A9 in a fed-batch fermentation process to cope with demands for electrochemistry and to practice handling of the fermentation and purification processes.

3.2.1. Fermentation

The fermentation of BaLac batches was performed in parallel under the control of a single controller. Hence, the course of the fermentation was similar for the three productions. For better presentation, only one fed-batch monitoring is shown in the figure, clone T383I (1A7) is described in figure 6.

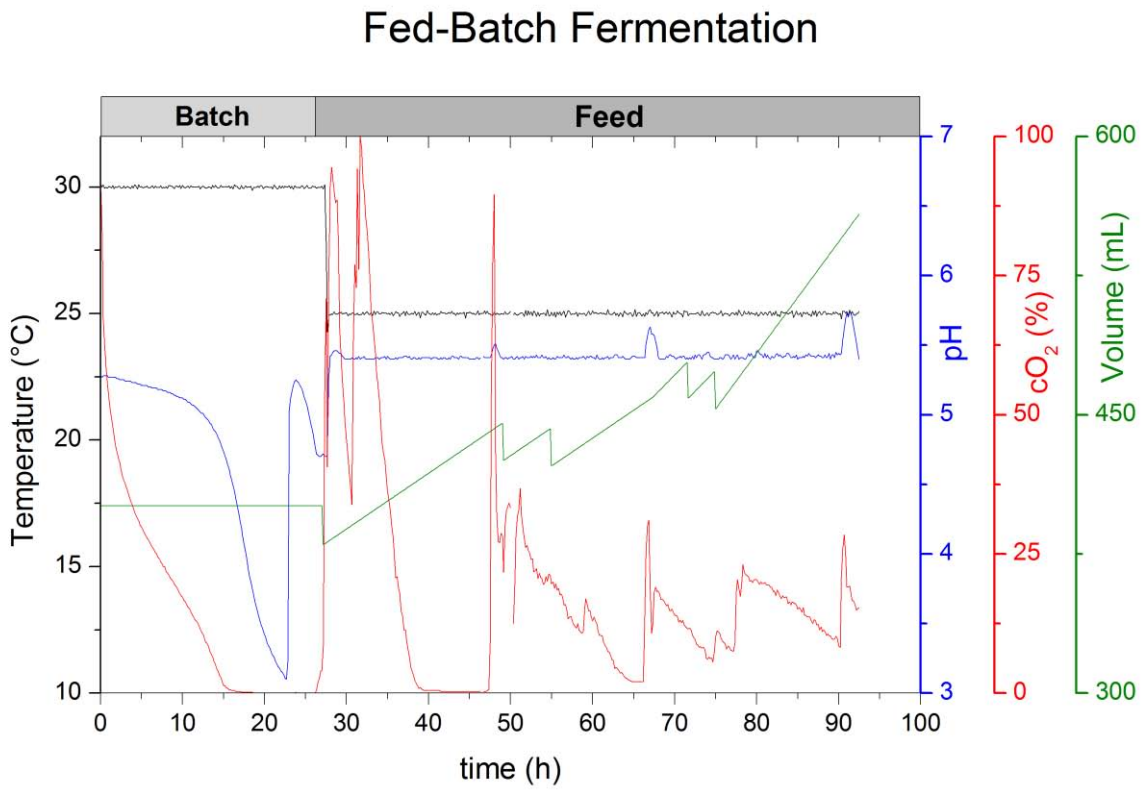

Figure 14: Graph of the fed-batch fermentation of BaLac T383I (1A7). Temperature (°C), pH, cO_2 (%) and volume (mL) are displayed on the various y-axis. 26 h of batch phase were followed by 68 h of glycerol feed phase. Samples were collected from the suspension after 27 h, 49 h, 55 h, 71 h, 75 h and 94 h. The productions of BaLac T383I (2A6) and BaLac T383I I424M (1A9) were carried out in parallel in a Multifors system.

At several time points, homogeneous 20 mL samples were drawn to allow monitoring of wet biomass (CWW), soluble protein content and laccase activity (ABTS).

A rise in cO_2 after 26 h indicated the end of the batch phase. For the 68 h feed phase, the temperature was decreased from 30 °C to 25 °C and ventilation was continued with pure oxygen.

An initial error in the base pump resulted in establishment of an acidic environment to reach a pH of circa 3.2. The pH was automatically balanced to pH 5.5 after re-adjusting the pump. During the feed phase, aeration limitations were reacted upon by manually increasing oxygen supply and stirring. Substrate feeds were escalated as projected.

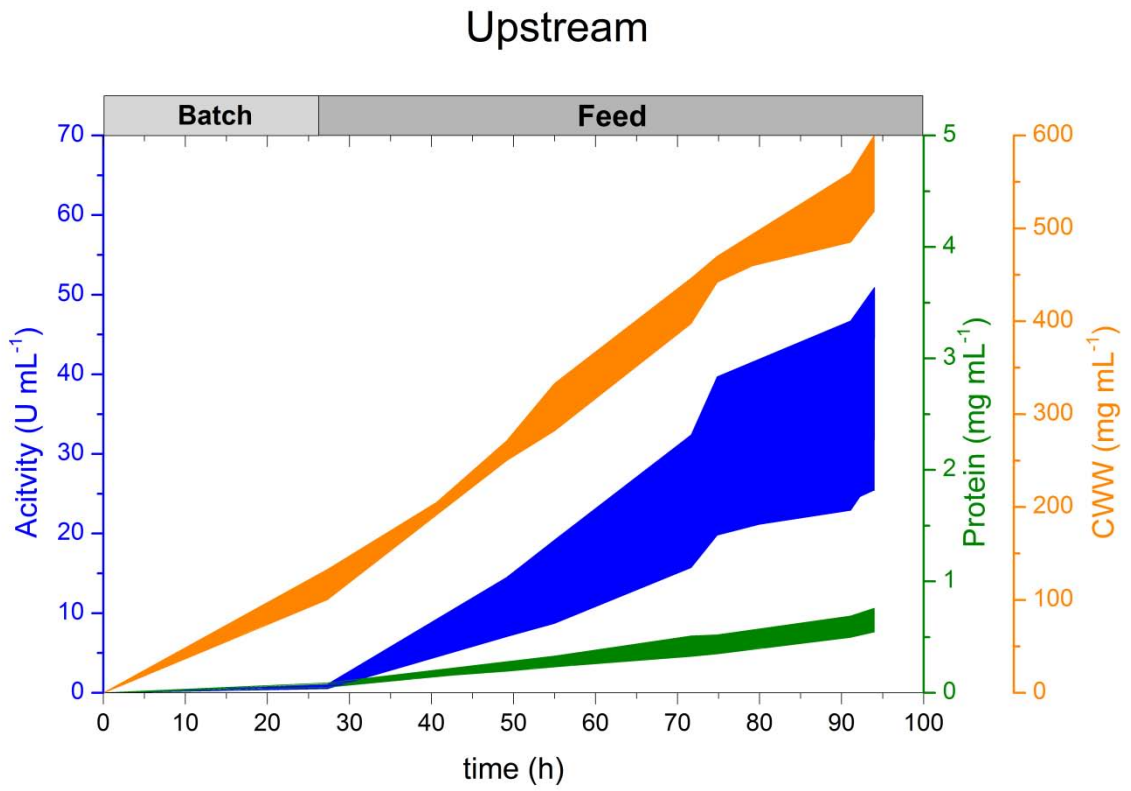

Figure 15: Graph of the increase in protein content (mg mL^{-1}, green), cell wet weight (mg mL^{-1}, orange) and activity (U mL^{-1}, blue) of the three clones during fermentation. The course of fermentation of all three productions can be found within the borders of the distinct areas. The batch phase of the fermentation was ended after 26 h and feed phase carried out for another 68 h, as stated in grey on the top of the figure.

The batch phase was ended with a cell wet weight of 133 mg mL^{-1}, a soluble protein content of 0.26 mg mL^{-1} and a laccase activity of 1.1 U mL^{-1}. During the feed phase, an increase in wet biomass to 519 mg mL^{-1} could be reached whilst the soluble protein content escalated to 0.76 mg mL^{-1} and the laccase activity to 50.9 U mL^{-1}, respectively. It was decided to stop the production process after circa 94 hours since no further increase in laccase content was detectable.

In Figure 15, one can note that the volumetric activities of the variants vary to a larger extent (represented by the blue area) whereas protein concentrations are relatively constant. This results in different specific activities (U $mg^{-}1$) and might be attributed to the accumulation of larger amounts of inactive enzyme or other protein impurities.

3.1.2. Purification

The fed-batch production yielded 520 mL of culture broth for each production. From that, 300 to 330 mL of clear enzyme rich culture supernatant could be harvested.

The subsequent ammonium sulfate precipitation allowed removing undesired protein content from the supernatant without compromising the yield. Yields of 96 % and higher are reported. After two consecutive stages of hydrophobic interaction chromatography HIC, final yields of 19-30 % could be obtained. The purification procedure managed to increase the specific activity to 182 U mg^{-1} and more. Purification schemes for the mentioned variants are given in table 13.

Table 13: Summary of purification data. Data were collected for the three clones T383I (1A7), T383I (2A6) and T383I I424M (1A9) and comprised total activity [U],specific activity [U mg^{-1}] total protein [mg],volume [mL], a purification factor and the yield [%].

Purification	Total activity [U]	Total protein [mg]	Volume [mL]	Specific activity [U mg^{-1}]	Purification factor	Yield [%]
T383I (1A7)						
Supernatant	24887	282	330	88	1.0	100
(NH4)2SO4	24224	271	350	90	1.0	97
HIC I (PSe)	18132	72	40	251	2.8	73
HIC II (PSo)	4762	17	3	273	3.1	19
T383I (2A6)						
Supernatant	14421	221	330	65	1.0	100
(NH4)2SO4	14203	217	350	65	1.0	98
HIC I (PSe)	12220	71	33	171	2.6	85
HIC II (PSo)	4259	19	2.5	222	3.4	30
T383I I424M (1A9)						
Supernatant	11487	183	300	62.7	1.0	100
(NH4)2SO4	11030	180	315	61.2	1.0	96
HIC I (PSe)	10552	69	32	153.5	2.8	92
HIC II (PSo)	2793	15	3	182	3.1	24

For the final protein solutions, protein concentrations were re-determined from fresh sample by spectrophotometric analysis at 610 nm since deviating results for the Bradford method were reported previously. The absorption peak at 610 nm is characteristic for the active laccase enzyme.

The values were quite significantly differing from the ones obtained by staining with the Bradford reagent and spectro-photometrical analysis at 280 nm.

T383I (1A7): 94.2 mg mL^{-1} (5.8 mg mL^{-1}) $^{280\ nm}$

T383I (2A6): 50.4 mg mL^{-1} (7.7 mg mL^{-1}) $^{280\ nm}$

T383I I424M (1A9): 76.6 mg mL^{-1} (5.1 mg mL^{-1}) $^{280\ nm}$

3.1.3. SDS PAGE

The subsequent analysis of purities by SDS PAGE confirmed the high performance of the purification procedure. The samples were compared to reference, a purified enzyme solution of the T383I I424M BaLac that was produced in a similar fashion previously.

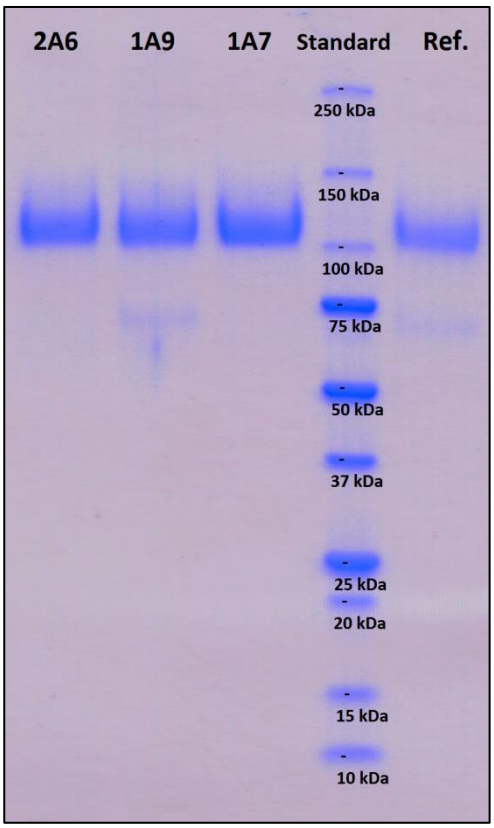

It is observable that the bands of the various laccase samples are comparable in position and intensity. Samples and reference can be found at circa 110 kDa. The difference to the theoretical size of 61.6 kDa that was calculated from the protein sequence can be attributed to the glycosylation. In the band of the 1A9 production, small amounts of protein impurities are to be found at circa 70 kDa. This has been reported for recombinant laccase fermentations and purifications before. It is assumed that these bands stem from partly unglycosylated enzyme that is immaturely released from the cells interior upon cell lysis. This can indicate production under suboptimal conditions.

Figure 16: SDS PAGE of enzyme productions T383I (1A7, 2A6) and T383I I424M (1A9). 13 µl of sample diluted to 0.15 mg mL^{-1} were loaded alongside 10 µL unstained precision plus protein standard and a reference of the same concentration. Separation was carried out at 120 V for 60 minutes prior to staining.

3.1.4. Discussion

The fed-batch fermentation protocol allowed for the production of sufficient amounts of laccase sample with an efficient and straight-forward approach. The subsequent multi-stage HIC purification procedure yielded sufficient amounts of enzymatic sample of decent concentration and highest purities, which has been confirmed by SDS-Page.

The difference in final protein concentrations which were determined the Bradford method and spectro-photometrical analysis at 610 nm may root in the relatively large error of the measurement that was amplified by dilutions of up to 1:10 000. Still, differences of up to a 5-fold were experienced before.

3.1. Cyclic voltammetry

The complete set of BaLac clones was assessed alongside the wild type to compare electrochemical midpoint potentials and the effect of different kinds on mutations on it. One should be aware that, as stated before, this collection of variants comprises positional mutations in diverse areas of the enzyme as well as different combinations of those.

3.1.1. Estimating midpoint potentials E_m

As was described previously, initial CV measurements were performed to test and develop the appropriate experimental setup and to detect potential outliers. All ten clones were analyzed in CV measurements. While the outcome of all experiments is regarded to be successful, the various CV plots did deliver magnificent dissimilarities in the degree of displaying electron transfer.
The plots were produced in Origin Pro 8.6. For each CV analysis of enzymatic sample overlays containing its blank and a first derivative of the reductive CV curve were produced. The first derivative of the reductive curve was added to improve demonstration of the steepest descents of the curve. Alignment of sample and blank curve via data processing was not regarded necessary since all sample CVs featured good correlation of shape and slope.

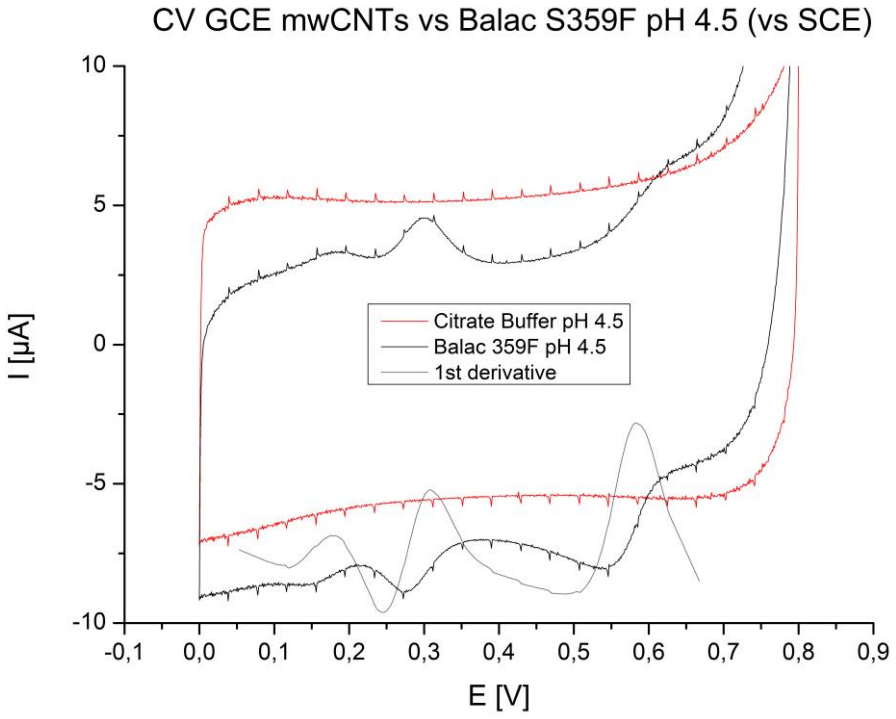

Figure 17: Mediatorless CV plot of BaLac variant S359F in 0.1 M citrate buffer (pH 4.5) measured at 25 °C on a glassy carbon electrode (GCE) with multi wall carbo nanotube coating (mwCNT) according to 2.11.3. The obtained CV curve from enzymatic sample (black) was compared to the blank (red). A first deviation of the reductive CV curve was calculated to facilitate evaluation. The electrode potentials are stated versus standard calomel electrode (SCE). Ramping: 0.8 V – 0.0 V – 0.8 V in two cycles at a scan rate of 0.01 V s^{-1}.

Figure 17 depicts a well pronounced non-turnover (i.e. without substrate) cyclic voltammogram for the BaLac variant S359F under aerobic conditions at 25 °C. As is observable above, the graph displays three peak couples in different potential windows. In addition to that, there is a notable shift in baseline current detectible that is attributed to the double-layer-capacitance of the enzyme on the electrodes surface. The Faradic signals result from electron transport to specific redox active centers in the laccase enzyme. Interestingly, the peak couples situated at approximately 0.15 V and 0.28 V vs SCE show comparable shape and area under curve (AUC) and a reversible re-oxidation. In contrast, the residual couple positioned between 0.55 V and 0.65 V vs SCE is remarkably unequal in area, indicating asymmetrical electron transfer at this center.

Midpoint potentials $E_{m;\ pH\ 4.5}$ of the electroactive redox centers were estimated by determining the potential at the peak maxima of the first derivatives. To specify, the redox center located at an electrode potential of 0.55 to 0.65 V vs SCE, the center located at circa 0.28 V vs SCE and the one located at circa 0.15 V vs SCE were referred to as "*High Potential Center*", "*Medium Potential Center*" and "*Low Potential Center*" respectively. The resolution in most voltammograms was not sufficient to detect Low Potential Centers. Hence they were not taken into account in the summary of Table 14.

Table 14: Summary of electrochemical midpoint potentials approximated from CVs in 0.1 M citrate buffer pH 4.5. Midpoint potentials of High Potential Centers (HPC) and Medium Potential Centers (MPC) are stated as potentials against SCE and NHE (NHE = SCE +0.244 V).Three different batches of variant T383I were evaluated to value reproducibility. The margin of error for this measurement is assumed to be circa ± 0.020 V.

	wt		T383I		T383I I424M	T383I A180D	T383I I491N	I424S	I424G	D236E	S359F	I491F	L499F
vs. SCE													
HPC	0.562	0.558	0.559	0.559	0.550	*n.d.*	*n.d.*	0.545	0.563	0.555	0.583	0.600	0.570
MPC	0.314	0.311	0.314	0.312	0.316	0.310	0.315	0.315	0.311	0.313	0.309	0.310	0.309
vs. NHE													
HPC	0.806	0.802	0.803	0.803	0.794	*n.d.*	*n.d.*	0.779	0.807	0.799	0.827	0.844	0.794
MPC	0.558	0.555	0.558	0.556	0.560	0.554	0.559	0.559	0.555	0.557	0.553	0.554	0.560

Notes: "*n.d.*" not determined indicated data was not of sufficient quality to allow for a statement

The introduced data suggests that MPCs are relatively conserved throughout the BaLac variants, as all can be found in a comparatively narrow range around 0.557 mV vs NHE (0.313 V vs SCE). Opposed to that, HPC values are fairly variable and are to be found between 0.779 V vs NHE (0.545 V vs SCE) and 0.844 V vs NHE (0.600 V vs SCE).

- MPC: mean = 0.557 V vs NHE (± 0.002 V), span = 0.007 V, n = 13
- HPC:, mean = 0.805 V vs NHE (± 0.017 V), span = 0.065 V, n = 11

Furthermore, comparison of three T383I samples indicates a reasonable reproducibility.
In order to further investigate the connection of HPC/MPC potentials to mutational aberrations and to get first insights in the differences of HPCs and MPCs in terms of pH dependence, data processing was used to set up summarizing graphs.

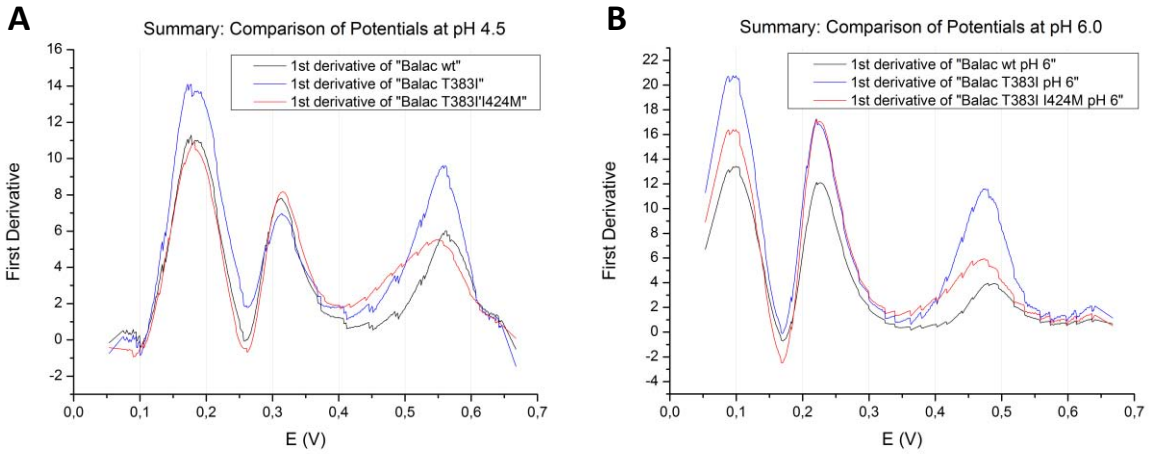

Figure 18: Overlay of first derivatives of the reductive CV curves of BaLac variant T383I I424M and those of its ancestors T383I and *wt*. Curves origin from CV experiments in different McIlvain buffers. The buffer was set to pH 4.5 in (A) to pH 6.0 in (B). For the gathering of curves, no alignment was performed. The peaks in the figure indicate the steepest local decent of the reductive curves and are not representative for midpoint potentials (potential E is stated versus SCE).

The depicted comparison shows a remarkable similarity of size and shape of LPC and MPC peaks independent from pH values. In contrast to that, the HPC peaks are characterized by increased variety. One can also observe the differences in HPC peak area (AUC) between pH 4.5 and pH 6.0 samples especially when being compared relatively to the respective LPC and MPC AUCs.
Analysis of the x-axis reveals a pH depended shift of peak maxima towards lower values with increasing pH. This shift appears to be unequal for HPCs and MPCs.

- pH 4.5: LPC (0.190 V) | MPC (0.320 V) | HPC (0.550 – 0.560 V)
- pH 6.0: LPC (0.090 V) | MPC (0.220 V) | HPC (0.470 – 0.480 V)

For the *wt* sample, the HPC peak derived from the pH 4.5 sample strongly differs from the pH 6.0 sample. Opposed to that, the derivative curves of variants T383I and T383I I424M resemble each other to a greater extend for both pH values. It is still yet to discuss if these properties are manifest and if they might be attributed to the mutational changes of the enzyme.

3.1.2. Investigations of pH dependence of E_m

The BaLac variants T383I and I424G were selected to be assessed in the pH experiment since both did show reliable signals in CV trials at pH extremes of pH 2.5 and pH 7.0 (see 2.11.4 for details). Furthermore, the clones contained mutations located in different functional regions of the enzyme,

at mutational positions known to account for altered stability (T383I) and shifted pH profile (I424M). Therefore they were regarded sufficiently diverse, hence perfectly suitable models to test pH dependence of E_m. For both samples, optimal results could be obtained from CVs at pH 4.5 though.

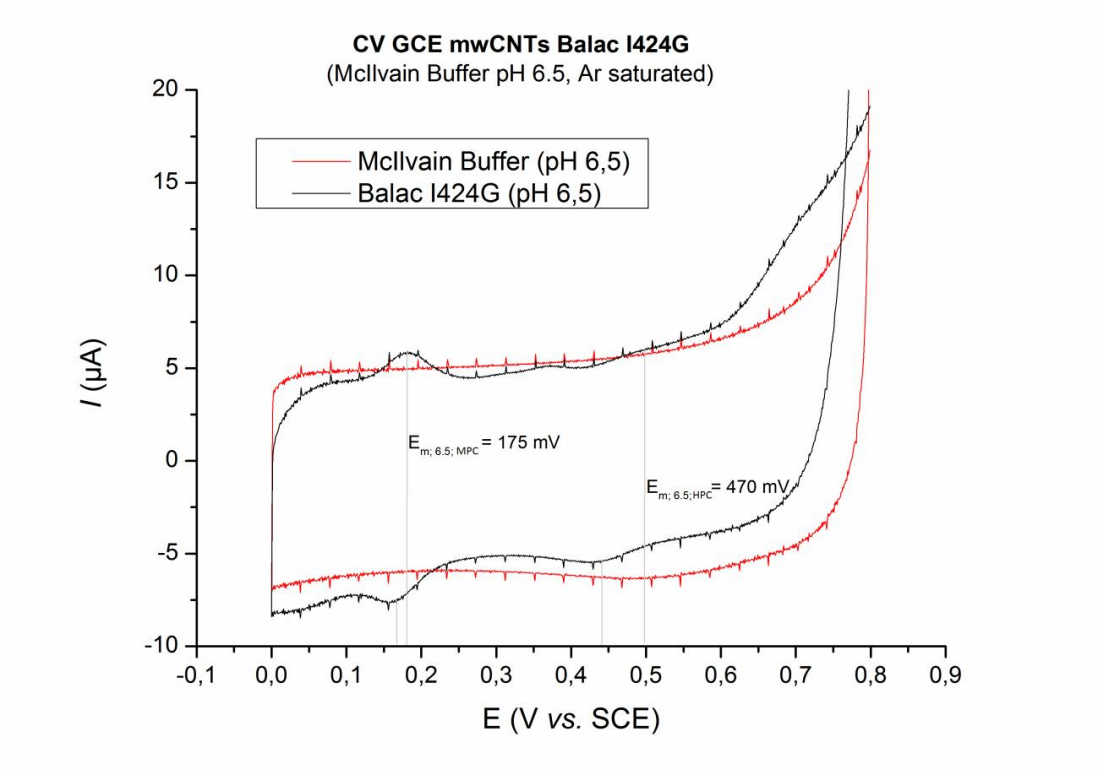

Figure 19: Mediatorless CV of BaLac I424G. The experiment was performed under anaerobic conditions (argon saturated McIlvain buffer pH 6.5) at 25°C. The blank (red) was again recorded versus enzyme free buffer. Electrode and nanotube coating were identical for blank and sample measurement. The electrode potentials are stated versus standard calomel electrode SCE (NHE = SCE + 0.244 V). Ramping: 0.8 V – 0.0 V – 0.8 V in two cycles at a scan rate of 0.01 V s^{-1}.

Differently from the procedure described before, midpoint potentials of MPC and HPC were now calculated by averaging the corresponding peak maxima of reductive and oxidative curve. No alignment was performed since blank and sample voltammograms expressed similar and overlapping profiles. The change of slope that is accounted to the increasing double layer capacitance current was not corrected by data processing. The obtained E_m values are specified in the figure: $E_{m;\ 6.5;\ MPC}$ = 0.175 V and $E_{m;\ 6.5;\ HPC}$ = 0.470 V vs SCE. Due to the pH dependent shift of potentials, LPCs are not visible in the graph. In addition to that, the shape of the voltammogram is different from the equivalent of figure 17 which can be attributed to the differing pH. A high current can be observed at approximately 0.7 V vs SCE that most probably results from the non-enzymatic transformation of small amounts of molecular oxygen that were trapped in the electrode coating. The intensity of this signal was decreasing for each CV cycle. As is observable above, a relatively small peak can be found to be located on the oxidative curve at circa 0.380 V vs SCE. There is no explanation for the source of this signal yet. Furthermore, one should note that the shift of HPC signals between reductive and

oxidative direction is larger than the respective MPC couple. This might be an additional indication for unbalanced electron transport.

To arrange datasets for both samples, E_m values of CVs at pH 2.5, 3.5, 4.5, 5.5, 6.5, 7.0 and 7.5 were gathered in the following table.

Table 15: Summary of pH dependent midpoint potentials (E_m) calculated from CVs of BaLac I424G and BaLac T383I in McIlvain buffer pH 2.5, 3.5, 4.5, 5.5, 6.5, 7.0 and 7.5. E_m values of High Potential Centers (HPC) and Medium Potential Centers (MPC) are stated as potentials against SCE and NHE (NHE = SCE +0.244 V). The margin of error for this measurement is assumed to be circa ± 0.010 V.

pH	2.5	3.5	4.5	5.5	6.5	7.0	7.5	2.5	3.5	4.5	5.5	6.5	7.0	7.5
		T383I						**I424G**						
vs. SCE														
HPC	0.657	0.629	0.578	0.521	0.459	0.442	0.412	0.657	0.621	0.578	0.523	0.470	0.420	0.392
MPC	0.390	0.341	0.285	0.232	0.174	0.146	0.120	0.393	0.342	0.286	0.233	0.175	0.147	0.120
vs. NHE														
HPC	0.901	0.873	0.822	0.765	0.703	0.686	0.656	0.901	0.865	0.822	0.767	0.714	0.664	0.636
MPC	0.643	0.585	0.529	0.476	0.418	0.390	0.364	0.637	0.586	0.530	0.477	0.419	0.391	0.364

This summarizing table was the basis for the calculation of pH dependent change of E_m. Both data sets were processed in Origin Pro to yield best fit straight lines of HPC and MPC midpoint potentials. Subsequently, slopes were calculated from the linear fit to quantify the decrease of potential in units of mV per decade of H^+-ion concentration (pH).

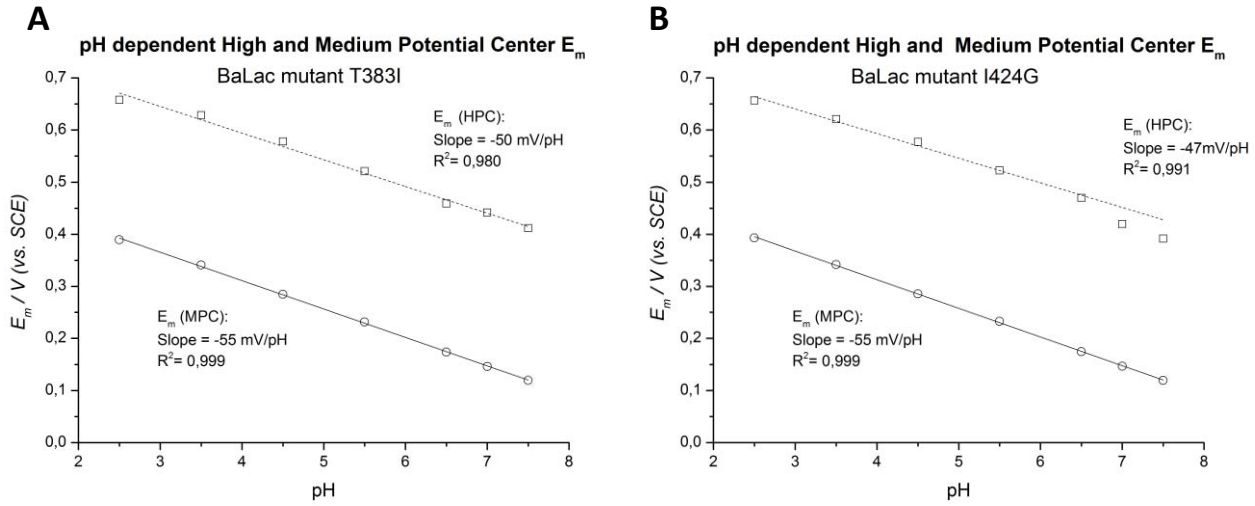

Figure 20: Shows plots of the midpoint potentials (E_m) of HPCs (squares) and MPCs (circles) of the BaLac variants T383I (A) and I424M (B). Assessment of E_m was performed at a series of different pH values. Data processing was used to create best linear fits for the data sets and to determine slope (given in units of mV per pH) and R^2. All potentials are stated versus SCE.

The evaluation of pH dependence of MPCs revealed remarkable linear behavior for the entire pH range of pH 2.5 to pH 7.5. This was the case for both variants as both displayed a steady decrease of

m = -55 mV/pH characterized by a coefficient of determination of R^2 = 0.999. Interestingly, this value comes relatively close to the theoretical value of RT/F = 59 mV for $\log_{10} a[H^+]/b[H^+] = 1$ that is determined by the Nernst equation at 25 °C.

Opposed to that, a linear fit for the HPC datasets is regarded to be suboptimal. As one can observe, the linear fit is predominantly defective at the ends of the scale. This is particularly true for BaLac I424G. The slopes are reported to be m = -50 mV/pH (R^2 = 0.980) and m = -47 mV/pH (R^2 = 0.991) for variant T383I and I424M respectively.

To make the whole concept of changing E_m related to changes in pH more comprehensive, the following plot was prepared.

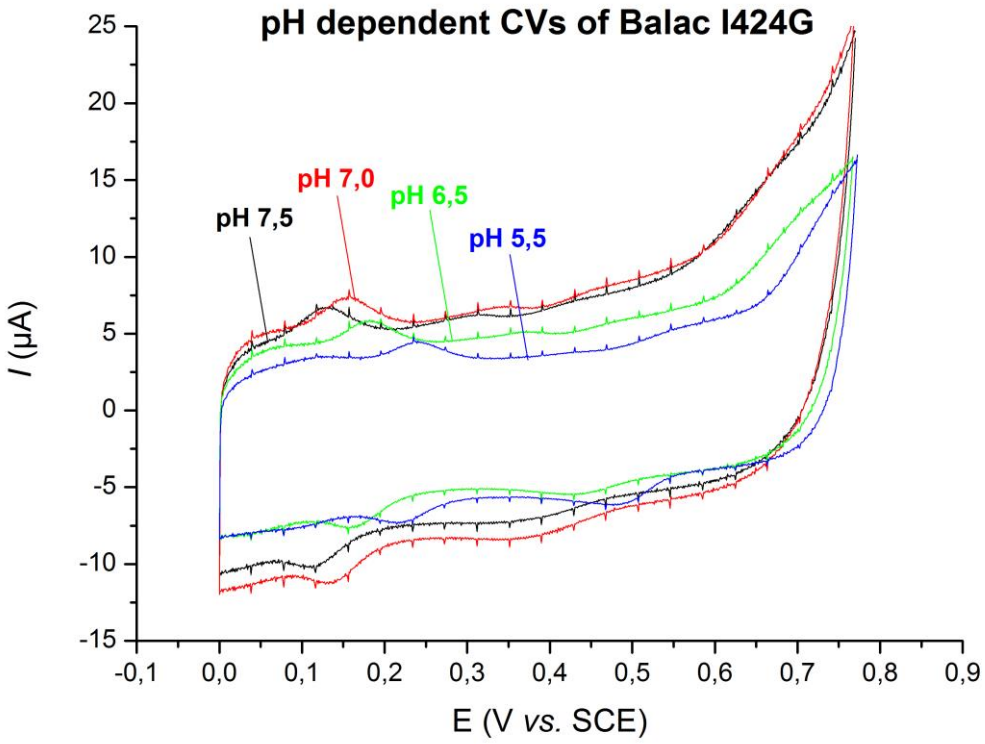

Figure 21: Overlay of mediatorless CV plots of BaLac I424G from experiments at pH 5.5 (blue), 6.5 (green), 7.0 (red) and 7.5 (black).

The positional changes of corresponding HPC and MPC peaks are very well detectible in the figure. In addition to that, one can observe the change in HPC reaction signal, equaling decreasing electron transport at this site with elevating pH.

3.1.3. Discussion

The initial approximation of E_m values by CV and subsequent determination of first derivatives of the reductive curves was necessary to proof the absence of outliers prior to spectro-electrochemical measurements. In addition to that, the analysis is regarded to allow for comparison among the set of variants despite the absolute E_m values might not be representative for native conditions.

It is still to deliberate about whether the various CV signals shall be accounted to HPC, MPC and LPC or whether association with the T1 and T2/3 copper centers of the laccase enzyme is appropriate. There is evidence to support that the presented HPC midpoint potentials of circa $E_{m;\,4.5}$ = 0.800 V are in agreement with previously described T1 site E_m values from CV experiments with high potential laccases (S. Shleev et al., 2005). Furthermore, the experienced electron transfer processes in this potential window express unequal current between reduction and re-oxidation and a relatively large peak separation. This has been identified to be a peculiar characteristic of the T1 copper and intramolecular electron transport in multi copper oxidases by others before (P. Ramírez et al., 2008)(S. Shleev et al., 2012)(C.H. Kjaergaard et al., 2015).

The obtained non-turnover Faradic signals in mediator-less CVs are in accordance with redox transformations that were reported to be corresponding to the laccases T1 site and T2/3 cluster (M. Frasconi et al., 2010). To the best knowledge of the author however, the detection of two separate and fully reversible signals (referred to as MPC and LPC signal) of the T2/3 cluster of a high potential laccase is novel. It may root in the presence of different intermediates of the T2/T3 site.

It could be shown that the T2/T3 cluster (MPC) E_m values are distributed over a relatively small range of 7 mV. In contrast, the T1 center potentials are to be found in an almost 10 times broader range of 65 mV. The accumulation of mutations close to the T1 site is likely to be the source for this increased diversity. The sensitive reaction of redox properties to mutational changes close to the T1 structure of the laccase enzyme has been reported before (E. Osipov et al., 2014).

The analysis of pH dependence reveals well pronounced linear relation of pH and the $E_{T2/3}$ values over a relative broad pH range. Changes of circa -55 mV per pH unit are in accordance with values proposed by the Nernst equation for H^+ dependent single electron transfers (A.J. Bard and L.R. Faulkner, 1980). Comparable $E_{T2/3}$ values were reported for the laccase relative bilirubin oxidase (BOx) (S. Shleev et al., 2012). Due to the linear association over the complete pH range, the influence of inhibitory molecules on the potentials $E_{T2/3}$ and E_{T1} is regarded as unlikely (F. Xu, 1997).

Aberrations from linear behavior can be found with the E_{T1} values of variant I424G. A decrease at pH 7.0 and 7.5 was observed. It is hypothesized that the insertion of a glycine at position 424 destabilizes the T1 coordination and involves an increased tendency for histidine deprotonation at a pH of 6.5 and higher. This then results in a decrease in E_{T1} potential due to the altered interaction of the T1 copper and its deprotonated coordinating partners His426 and His494. This phenomenon is not detectible for BaLac T383I which harbors the native T1 coordination. Thus, a difference in T1 potentials at pH 7.0 of $E_{T1;7.0}$ = 686 mV (T383I, native T1) compared to $E_{T1;7.0}$ = 664 mV of I424G is reported, see Table 15.

Recent findings by our group report the improved catalytic activity of variant I424G at neutral pH (BaLac I424G k_{cat} = 59.8 s^{-1}, BaLac *wt* k_{cat} = 40.1 s^{-1}) (unpublished). Furthermore, the outcome of an electrochemical analysis of BOx proposes the limitation of the catalytic turnover by intramolecular-electron-transfer (IET) in more alkaline milieus. This effect is explained by an uphill IET process from the Cu-T1 to the Cu-T2/3 cluster of the Box enzyme where variants with decreased T1 potentials (BOx M467Q E_{T1}=0.43 V, BOx *wt*: E_{T1}=0.67 V) were characterized by improved k_{cat} at neutral pH (S. Shleev et al., 2012). These data can support the idea that increased catalytic activity correlates with the decreased T1 potentials of certain *Botrytis aclada* laccase variants at neutral pH.

The problem of depletion of one or more copper atoms from the T2/3 site has often been reported (V. Ducros et al., 2001),(C. Bukh and M.J. Bjerrum, 2010).
It was shown in this work that cyclic voltammetry might be a probable method for the detection of the T2 copper in the trinuclear cluster. The non-turnover Faradic signals in voltammograms can potentially facilitate the analysis of copper content by comparison of peak areas.

CV peaks corresponding to the non-enzymatic reduction of oxygen to water on the electrode surface indicate the insufficient removal of molecular oxygen from the solution. It might be possible that small amounts of oxygen were trapped inside the nanotube coating during the preparation and were not completely removed during the flushing with argon.

The CV procedure that was developed in the course of this thesis presents itself as a simple, potent and robust method to investigate electrochemical properties of enzymatic samples. The carbo nanotube coating seems to be sufficient to resolve subtle electron transfer processes of oxidases like laccase via direct electron transfer. Good resolution of voltammograms can be reached with slow scan rates and as little as 5 µl of pure enzymatic sample. Also, analysis of potentials at neutral pH can be performed without exhibiting the sample to inhospitable environments for longer periods

3.2. Spectroelectrochemical studies

Midpoint potentials that were estimated via CV experiments were to be confirmed with mediated redox titration (MRT). This method relies on the spectroscopic property of the T1 copper to produce strong absorption bands at circa 600 nm wavelength when resting in an oxidized state. Mediatorless titration was tested as well. All potentials are stated vs NHE if not specified otherwise.

3.2.1. Mediated redox titration (MRT)

The whole set of BaLac variants was assessed as described in 2.11.5. The potentiometric titration curves were prepared from the collected data sets and were processed in Origin Pro. Absorbance spectra and Nernst plots were recorded in parallel and added to the evaluation.

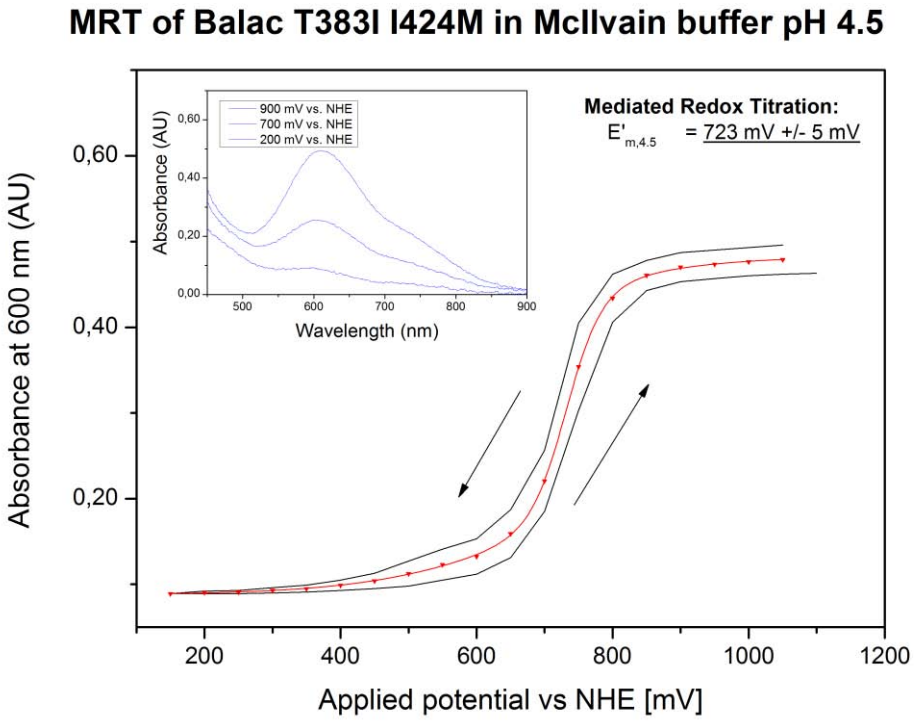

Figure 22: MRT of *Botrytis aclada* laccase variant T383I I424M in McIlvain buffer pH 4.5 at 25 °C. The potentiometric titration curves (top: reduction, bottom: oxidation) were averaged (red curve) in order to calculate midwave potentials $E_{m;4.5}$. Ramping: 1050 mV – 150 mV – 1100 mV vs NHE in steps of 50 mV per 5 min. Insert: Spectra from the titrations are corresponding to fully oxidized BaLac (900 mV), partially reduced BaLac (700 mV) and fully reduced BaLac (200 mV). The redox mediators, 200 µM $K_4[Fe(CN)_6]$, $K_4[Mo(CN)_8]$ and $K_4[W(CN)_8]$ are reported to be independent of scan direction and transparent above 500 nm.

This plot shows a well pronounced redox titration with a minimal discrepancy between reductive and oxidative curve. Both display similar profiles and are converging at the reductive end whilst forming well shaped plateaus at the respective ends. Data points were averaged at each potential and subsequently fitted to a sigmoidal curve with the help of OriginPro. E_m was determined from this fit at precisely mid distance from reductive to oxidative plateau, representing equal concentrations of

reduced and oxidized species ([Ox]/[Red] = 1). The margin of error roots from the operative setup mainly and is assumed to be ± 5 mV. For this sample, $E_{m;\,4.5}$ = 725 mV vs NHE is reported (data not shown). Nernst plots were prepared to gather basic titration parameters and to confirm the previously obtained half wave potentials.

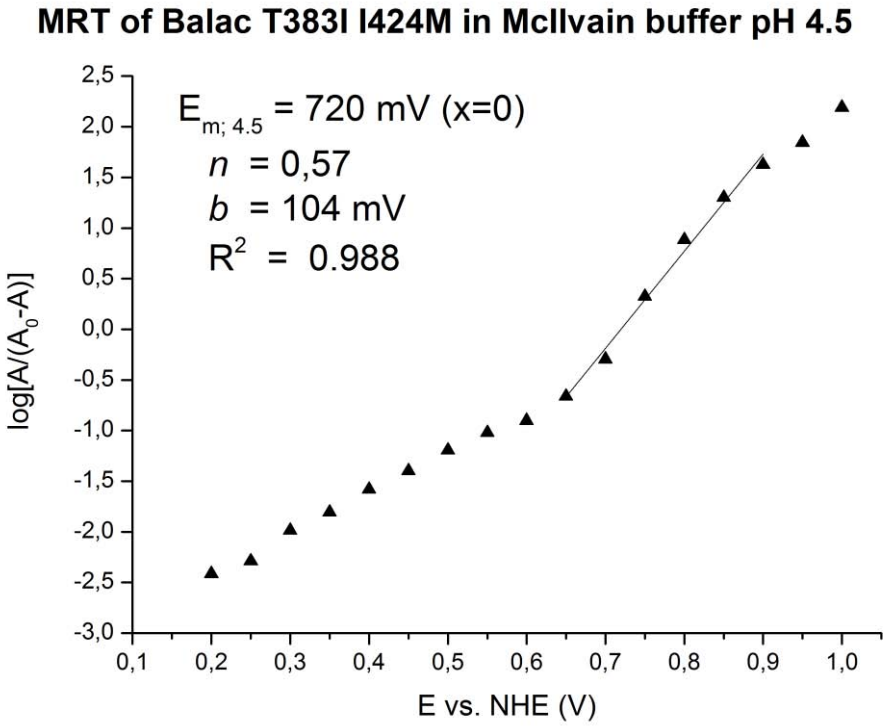

Figure 23: Nernst plot of BaLac T383I I424M MRT. The absorbance at 600 nm is dependent on the applied potential (E). The plot delivers basic titration parameters such as "b" (slope of the titration curve), n (number of electrons) and R^2 (correlation coefficient). It is also used to confirm the E_m. Note that Nernst plots are prepared with units in volts on the x-axis.

It is observable that the linear fit in the plot is compromised. This is thought to root in the extended titration that was performed to guarantee complete reduction of enzyme. In this part of the curve, logarithmic relation is biased. To still be able to calculate the titration parameters a least-squares linear regression analysis was performed for the main redox transition area of 0.6 V – 0.9 V. The linear correlation coefficient R^2 was reported to be higher than 0.98.

Notably, the E_m value obtained from the 600 nm Nernst plot (at x = 0): E_m = 720 mV vs. NHE matches the previously calculated of 725 mV ± 5 mV vs. NHE. The slope b was found to be b = 104 mV indicating n = 0.57 electrons being transferred.

The differences between reductive and oxidative titration are relatively small, 32 mV for this measurement, equaling less than 4 % of the scanning range of 0.9 V. The deviation in signal intensity at 600 nm between titration start (A_{600} = 0.496) and end (A_{600} = 0.462) proves the loss of blue color to some small extent. Coinciding of these data points is unlikely to appear though since enzyme stability

clearly is an issue during the three hour experiment. It is assumed that a complete Nernst equilibrium could be reached via scanning rates of 50 mV / 5 min.

Hence, the outcome of this set of MRT measurements is regarded as very valuable. Firstly, the obtained E_m values were basically independent of the direction of scanning. Secondly, it was able to reversibly cycle the enzymatic samples between their entirely oxidized and reduced form.

All BaLac variants were assessed in the MRT experiments. Again, three different batches of variant T383I were used in the course of this work to judge reproducibility. E_m values determined from Nernst plots and titration curves were averaged for the summary. The calculation of *"n"* and *"b"* is based on the Nernst equation (for a cell at 25 °C) and can be related to:

$$E = E^0 + \frac{0.05916}{n} \cdot log_{10} \frac{a_{Ox}}{a_{Red}} \qquad \frac{RT}{F} = 0.05916 = n \cdot b$$

The following data could be gathered:

Table 16: Summary of midwave potentials $E_{m;4.5}$ [V], slopes (b) [V], number of electrons (n) obtained from MRTs in McIlvain buffer pH 4.5 at 25 °C. Potentials were averaged from Nernst plot and titration curve and are stated vs NHE. Three different batches of variant T383I were evaluated to value reproducibility. The margin of error for this measurement is assumed to be circa ± 0.005 V. Titration: 1050 mV (oxidized BaLac) – 150 mV (reduced BaLac) – 1100 mV (re-oxidized BaLac) at a scan rate of 50 mV per 5 min. Mediated electron transport with 200 µM redox mediators K4[Fe(CN)6], K4[Mo(CN)8] and K4[W(CN)8].

	wt	T383I			T383I I424M	T383I A180D	T383I I491N*	I424S	I424G	D236E	S359F	I491F	L499F
Nernst	0.719	0.735	0.751	0.753	0.720	0.712	0.565	0.756	0.682	0.743	0.740	0.690	0.667
Titration	0.723	0.737	0.750	0.753	0.725	0.719	0.564	0.764	0.697	0.747	0.745	0.688	0.672
E_m (avg.)	0.721	0.736	0.751	0.753	0.723	0.716	0.565	0.760	0.690	0.745	0.743	0.689	0.670
n	*0.42*	*0.51*	*0.55*	*0.57*	*0.57*	*0.53*	*0.53*	*0.63*	*0.64*	*0.52*	*0.52*	*0.35*	*0.51*
b	*0.140*	*0.115*	*0.106*	*0.103*	*0.104*	*0.111*	*0.112*	*0.093*	*0.092*	*0.113*	*0.113*	*0.170*	*0.116*

Notes: "*" BaLac T383I I491N displayed irregular behavior in the MRT measurements. The reduction happened in two separate steps; subsequent re-oxidation was biased and did not lead to the initial signal. Furthermore, a shift of absorbance maximum was observed (data not shown). Measurement was repeated and led to the same results.

As is observable in Table 16, the $E_{m;4.5}$ values for the set of variants are reasonable and relatively uniform as all values are located between $E_{m;4.5}$ = 0.670 V (BaLac L499F) and $E_{m;4.5}$ = 0.760 V (BaLac I424S). Reproducibility is assumed to be satisfactory when regarding the obtained data of T383I measurements. The presented data set can be described as follows (BaLac T383I I491N neglected):

- $E_{m;4.5}$ (T1): mean = 0.725 V vs NHE (± 0.029 V), span = 0.090 V, n = 12

The values for *"n"* are reasonable as well and can theoretically be n = 1 for slopes of b = 0.05916 V. One should understand that *"n"* and *"b"* are parameters to describe the practical electron transport between enzyme and electrode and are specific for each titration and enzyme.

3.2.2. Direct electron transfer redox titration (DRT)

Trials of direct electron transfer (DET) titrations were performed with selected variants. No redox active mediators were added to the sample and enzymes were again assessed on a bare gold electrode. Aside from the mediators, the procedure was identical to the previously described MRT procedure.

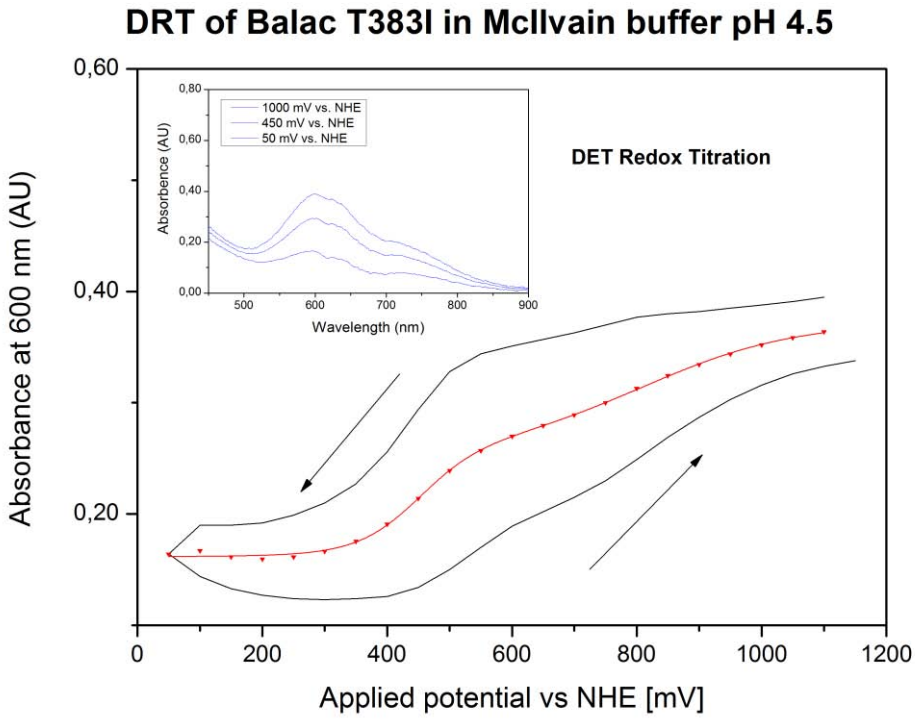

Figure 24: A direct electron transfer redox titration (DRT) trial of *Botrytis aclada* laccase variant T383I in McIlvain buffer pH 4.5 at 25 °C. The potentiometric titration curves (top: reduction, bottom: oxidation) were averaged (red curve). Ramping: 1100 mV – 50 mV – 1150 mV in steps of 50 mV per 5 min. Insert: Spectra from the titrations are corresponding to fully oxidized BaLac (1000 mV), partially reduced BaLac (450 mV) and almost fully reduced BaLac (50 mV). No redox mediators were added.

Obviously, the DRT trial showed magnificent differences to the MRT experiments. For the first 600 mV only little reduction is displayed. Thereafter, increasing reduction appears. The subsequent re-oxidation maintains a relatively slow turnover of laccase molecules for the whole range.
In addition to that, the curves seem to be separated by several hundreds of millivolts for most of the range, indicating slow electron transport. It was resigned to calculate the major titration parameters since this trial was regarded a proof of principle study.

3.2.3. Discussion

The E_m values that were obtained by spectroelectrochemical investigation in this work conform to previously published potentials for high redox potential multicopper oxidases (S. Shleev et al., 2005), (O.V. Morozova et al., 2007). Data that have been recently published for MRTs of *Botrytis aclada* laccase wild type suggest an $E_{m;5.5}$ of 0.720 V vs NHE (E. Osipov et al., 2014). Despite different buffers were used, this comes very close to the BaLac wild type MRT from this work, where $E_{m;4.5}$ was reported to be 0.721 V vs NHE.

Interestingly, E. Osipov (E. Osipov et al., 2014) mentions a position L499M mutational variant, characterized by $E_{m;5.5}$ = 0.580 V vs NHE. Another clone to contain a mutation at this position was stated in this work: BaLac L499F. Its $E_{m;4.5}$ was found to be 0.670 V vs NHE. Seemingly, the exchange of a leucine residue to methionine has more severe influences on the potential than the exchange to a phenylalanine residue by providing sulfur in close vicinity as a good ligand for the copper. This can be supported by another mutational couple that was analyzed via MRT in this work: BaLac I424S and I424G. In comparison to the wild type, variant I424G has a slightly reduced $E_{m;4.5}$ of 0.690 V vs NHE. This is comprehensible since both amino acids have common chemical properties. The exchange of isoleucine to a hydrophilic serine is reported to remarkably increase the potential from $E_{m;4.5}$ = 0.721 V to $E_{m;4.5}$ = 0.760 V vs NHE. When further comparing the BaLac variants one will note the nearly identical titration parameters of n = 0.63, n = 0.64 for clone I424S and I424G respectively. As mentioned before, it has been shown that this position was identified to have sensitive effects on the pH profile of the enzyme with certain substrates (E. Breslmayr, 2015, unpublished).

In the case of BaLac T383I I491N, there is no explanation for the atypical behavior in the MRT yet. Presumably, the reduction of the T1 site correlates with partial restructuration that cannot be restored during re-oxidation. This appears to be a distinct feature of the I491N mutation. The exchange of a hydrophobic isoleucine residue to a hydrophilic asparagine residue is thought to have tremendous impact in every case (MRT plot in appendix).

Obviously, the data obtained from CV measurements and MRT measurements are not coinciding by means of absolute values and relative differences. This is not surprising as different procedures on different electrode materials most probably will lead to variable results. Explanations for that may source in the different orientation of the enzyme on the electrode surfaces and as a result the different intramolecular direction of electron transfer in the enzyme (P. Ramírez et al., 2008). In addition to that, the availability of oxygen in the measurement cell, the absence of redox mediators

in CV experiments and the different distance of responsive copper atoms to the electrode might as well influence the results.
Nevertheless, the span of E_{T1} values at pH 4.5 of 65 mV and 90 mV for cyclic voltammetry and MRT respectively are comparable and thought to be relatively small when considering the large set of diverse variants. The mutation of the sites I424 (S: E_{T1} + 39 mV vs. *wt*, G: E_{T1} - 31 mV vs. *wt*), I491 (F: E_{T1} - 32 mV vs. *wt*) and L499 (F: E_{T1} - 51 mV vs. *wt*) seemed to be of greater importance for the E_{T1}.

This study shows further, that DET is possible between laccases and bare gold electrodes although high currents cannot be expected due to the compromised speed of electron transfer. Comparable data have been published for bilirubin oxidase before (A. Christenson et al., 2006)
In the DET titration, faster electron transport was evident when the potential reached values lower than approximately 500 mV. I here suggest that in experiments with the gold electrode, the T2/T3 site is closer positioned to the surface and acts as a circa 500 mV barrier to hinder electrons to travel from the T1 site to the electrode when redox mediators are absent. Only when the applied potential reaches values of 500 mV or lower electrons are able to overcome the T2/T3 (E_m ca. 500 mV) and travel to the T1 (E_m ca. 720 mV) where they can reduce the Cu^{II} and hence diminish the blue color (Figure 5). The results of the DET measurement therefore support the orientation of blue copper oxidases on gold electrodes that was suggested by P. Ramirez et al (2008) and the T2/T3 potentials that were estimated by CV during this work.

One should keep in mind that the age of the samples might be partly contributing to the electrochemical measurements since the depletion of the Cu2 is detrimental for the redox properties.

4. Conclusion

The third iteration of the directed evolution experiment that was using the T383I I424M variant as a template unfortunately failed to isolate new variants. It also did not provide any novel information about positions in the protein that are influencing the targeted features of the laccase.

A successful production procedure including a straightforward fed-batch fermentation and a two stage HIC purification managed to yield sufficient enzyme of highest purities.

The subsequent electrochemical characterization of ten engineered BaLac variants by CV and electrochemical redox titration revealed valuable information about the redox properties of the laccases. These measurements managed to determine midpoint potentials of the laccase's T2/T3 ($E_{T2/T3}$) and T1 (E_{T1}) potentials. Positions like the I424, I491 and I499 seem to be vital for the E_{T1}. On the contrary, the T383I mutation responsible for improved stability of the enzyme was reported to have no effect on the E_{T1}. In addition to that, the DET between laccases and bare gold electrodes was confirmed.
A novel CV setup was developed in the course of this work that presents itself as a potent and robust method to investigate electrochemical properties with just little sample. The pH dependence of potentials was evaluated in a separate series of CV experiments. It proposed a possible influence of histidine deprotonation on the redox potential and the likelihood of beneficial effects of decreased potentials to improved catalytic activity at neutral pHs in particular.

The information gained might assist in improving our understanding of the electrochemical nature of laccases and the group of multicopper oxidases. It can support suggestions that have recently been published.

Outlook

Computational modeling and simulation of selected BaLac variants could facilitate the elucidation of structural influences to the redox potential in future work. Especially when adding T2/T3 mutations to the collection of variants valuable knowledge could be obtained.

5. Appendix

5.1. MRT plot of BaLac T383I I491N

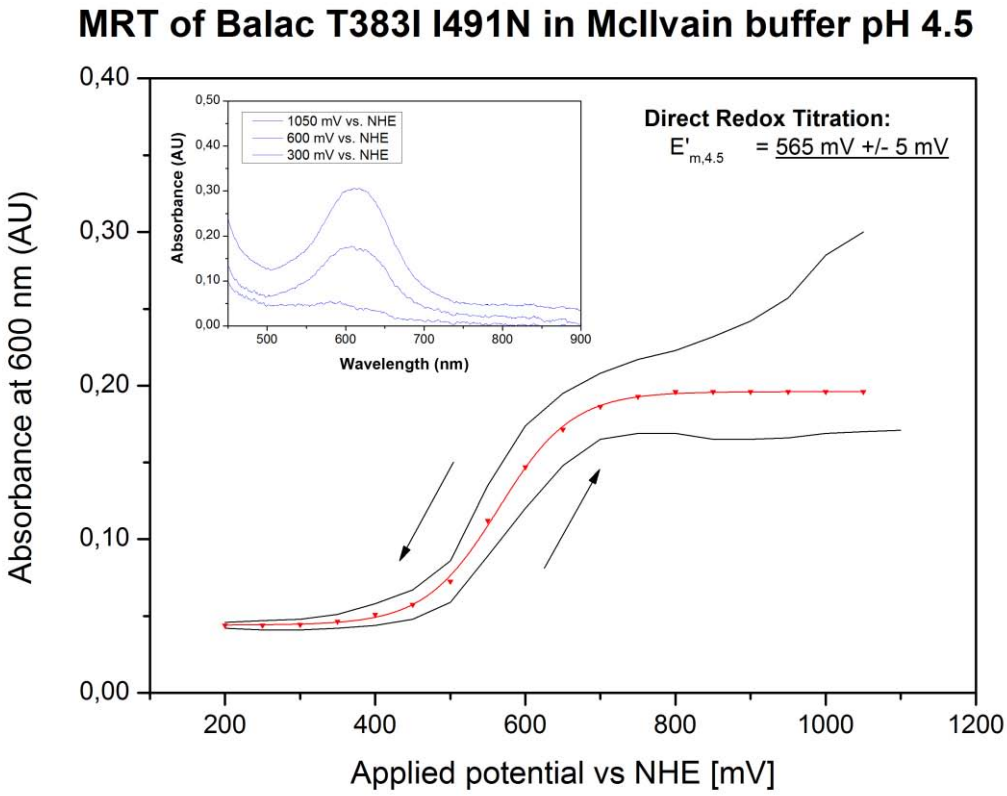

Figure 25: MRT of *Botrytis aclada* laccase variant T383I I491N in McIlvain buffer pH 4.5 at 25 °C. The potentiometric titration curves (top: reduction, bottom: oxidation) were averaged until 800 mV vs NHE (red curve) in order to calculate midwave potentials $E_{m;\,4.5}$. The averaging was continued till 1050 mV vs NHE by keeping the curve constant. Ramping: 1050 mV – 200 mV – 1100 mV vs NHE in steps of 50 mV per 5 min. Insert: Spectra from the titrations are corresponding to fully oxidized BaLac (1050 mV), partially reduced BaLac (600 mV) and fully reduced BaLac (300 mV vs NHE). The redox mediators, 200 µM $K_4[Fe(CN)_6]$, $K_4[Mo(CN)_8]$ and $K_4[W(CN)_8]$ are reported to be independent of scan direction and transparent above 500 nm.

5.2. List of figures

5.3. List of tables

5.4. Sequences

Botrytis aclada laccase nucleotide sequence from cDNA:

```
   1 ATGAAGTATT TCACAGTCTT TACTGCCCTC ACTGCATTAT TTGCACAGGC CTCTGCATCA
  61 GCTATTCCAG CTGTTCGTTC AACACTCACT CCTCGTCAAA ATACCACTGC CTCTTGTGCA
 121 AACTCAGCTA CTTCCAGATC TTGCTGGGGA GAGTATTCCA TTGATACCAA CTGGTATGAT
 181 GTTACTCCTA CAGGAGTCAC CAGAGAATAC TGGCTTTCAG TTGAGAATTC TACCATCACA
 241 CCTGATGGTT ATACTCGCTC AGCCATGACT TTCAATGGAA CTGTTCCGGG ACCAGCAATT
 301 ATAGCAGACT GGGGTGACAA TCTTATAATC CACGTTACCA ACAATCTTGA ACACAACGGT
 361 ACATCTATTC ACTGGCATGG AATTCGTCAA CTAGGAAGTC TCGAATACGA CGGTGTACCC
 421 GGTGTAACGC AATGTCCCAT CGCTCCTGGA GATACCTTGA CCTACAAGTT CCAAGTTACT
 481 CAATATGGAA CCACTTGGTA TCATTCTCAC TTCTCTCTTC AATACGGTGA TGGACTCTTT
 541 GGACCCTTGA TCATTAACGG TCCTGCTACT GCGGACTATG ATGAAGACGT TGGTGTAATT
 601 TTCCTCCAAG ATTGGGCACA TGAATCCGTT TTCGAAATTT GGGACACCGC TAGACTCGGC
 661 GCTCCCCCAG CACTTGAGAA CACTTTGATG AATGGAACCA ACACCTTTGA CTGCTCAGCT
 721 TCTACCGATC CTAACTGCGT TGGGGGTGGT AAGAAATTTG AGTTGACTTT CGTCGAAGGT
 781 ACCAAATATA GATTGAGATT GATCAATGTC GGAATTGACA GTCACTTCGA ATTCGCCATT
 841 GATAACCACA CACTTACTGT CATTGCCAAC GATCTTGTTC CAATTGTACC CTACACTACC
 901 GACACACTTC TCATTGGCAT TGGTCAAAGA TACGATGTCA TTGTTGAAGC CAATGCGGCA
 961 GCAGACAACT ACTGGATTAG AGGTAATTGG GGAACCACCT GCTCAACCAA CAATGAAGCA
1021 GCAAATGCTA CAGGTATCCT CCGATACGAT AGCTCCAGCA TCGCAAATCC TACCTCTGTT
1081 GGCACCACGC CCCGCGGTAC TTGCGAGGAT GAGCCGGTTG CCAGTCTTGT CCCACACTTG
1141 GCATTGGACG TTGGTGGATA CTCTCTCGTC GATGAACAGG TGTCCTCCGC ATTCACCAAC
1201 TACTTCACAT GGACCATCAA CTCAAGCAGT TTACTCCTCG ATTGGAGCTC CCCAACCACT
1261 CTCAAAATTT TCAATAATGA GACAATCTTC CCAACTGAAT ACAACGTTGT CGCTCTCGAG
1321 CAAACCAACG CTAACGAAGA GTGGGTCGTA TATGTCATCG AAGATCTCAC CGGCTTCGGC
1381 ATTTGGCATC CTATCCATCT CCACGGCCAC GATTTCTTCA TCGTAGCTCA AGAAACTGAT
1441 GTGTTCAATT CCGACGAGTC GCCAGCCAAG TTCAACCTTG TCAATCCTCC ACGTCGTGAC
1501 GTCGCGGCAC TTCCCGGAAA CGGTTATCTT GCCATTGCAT TCAAGCTTGA CAATCCTGGT
1561 TCATGGCTTC TTCATTGTCA TATCGCATGG CACGCATCTG AGGGGTTGGC AATGCAATTT
1621 GTGGAGTCTC AAAGCTCAAT TGCGGTCAAG ATGACCGACA CTGCTATATT TGAGGATACT
1681 TGTGCAAACT GGAATGCTTA TACTCCTACT CAATTGTTTG CTGAGGACGA TTCTGGAATT
1741 TAA
```

Botrytis aclada laccase amino acid sequence:

```
  1 MKYFTVFTAL TALFAQASAS AIPAVRSTLT PRQNTTASCA NSATSRSCWG EYSIDTNWYD
 61 VTPTGVTREY WLSVENSTIT PDGYTRSAMT FNGTVPGPAI IADWGDNLII HVTNNLEHNG
121 TSIHWHGIRQ LGSLEYDGVP GVTQCPIAPG DTLTYKFQVT QYGTTWYHSH FSLQYGDGLF
181 GPLIINGPAT ADYDEDVGVI FLQDWAHESV FEIWDTARLG APPALENTLM NGTNTFDCSA
241 STDPNCVGGG KKFELTFVEG TKYRLRLINV GIDSHFEFAI DNHTLTVIAN DLVPIVPYTT
301 DTLLIGIGQR YDVIVEANAA ADNYWIRGNW GTTCSTNNEA ANATGILRYD SSSIANPTSV
361 GTTPRGTCED EPVASLVPHL ALDVGGYSLV DEQVSSAFTN YFTWTINSSS LLLDWSSPTT
421 LKIFNNETIF PTEYNVVALE QTNANEEWVV YVIEDLTGFG IWHPIHLHGH DFFIVAQETD
481 VFNSDESPAK FNLVNPPRRD VAALPGNGYL AIAFKLDNPG SWLLHCHIAW HASEGLAMQF
541 VESQSSIAVK MTDTAIFEDT CANWNAYTPT QLFAEDDSGI
```

5.5. References

Arnold, F. H., and A. A. Volkov. 1999. “Directed Evolution of Biocatalysts.” *Current Opinion in Chemical Biology* 3 (1): 54–59.

Bard, Allen J., and Larry R. Faulkner. 2001. “Wiley: Electrochemical Methods: Fundamentals and Applications, 2nd Edition - Allen J. Bard, Larry R. Faulkner.”

Bistolas, Nikitas, Andreas Christenson, Tautgirdas Ruzgas, Christiane Jung, Frieder W. Scheller, and Ulla Wollenberger. 2004. “Spectroelectrochemistry of Cytochrome P450cam.” *Biochemical and Biophysical Research Communications* 314 (3): 810–16.

Bradford, M. M. 1976. “A Rapid and Sensitive Method for the Quantitation of Microgram Quantities of Protein Utilizing the Principle of Protein-Dye Binding.” *Analytical Biochemistry* 72 (May): 248–54.

Breslmayr, Erik 2015. *Engineering of a High Redox Potential Laccase towards Improved Performance at Physiologic Conditions*. 2015.

Bukh, Christian, and Morten J. Bjerrum. 2010. “The Reversible Depletion and Reconstitution of a Copper Ion in Coprinus Cinereus Laccase Followed by Spectroscopic Techniques.” *Journal of Inorganic Biochemistry* 104 (10): 1029–37. doi:10.1016/j.jinorgbio.2010.05.010.

Bullen, R. A., T. C. Arnot, J. B. Lakeman, and F. C. Walsh. 2006. “Biofuel Cells and Their Development.” *Biosensors & Bioelectronics* 21 (11): 2015–45. doi:10.1016/j.bios.2006.01.030.

Chilvers, Martin I. 2007. “Detection and Identification of Botrytis Species Associated with Neck Rot, Scape Blight, and Umbel Blight of Onion.” *Plant Health Progress*. doi:10.1094/PHP-2006-1127-01-DG.

Christenson, Andreas, Sergey Shleev, Nicolas Mano, Adam Heller, and Lo Gorton. 2006. “Redox Potentials of the Blue Copper Sites of Bilirubin Oxidases.” *Biochimica Et Biophysica Acta* 1757 (12): 1634–41. doi:10.1016/j.bbabio.2006.08.008.

Christopher, Lew Paul, Bin Yao, and Yun Ji. 2014. “Lignin Biodegradation with Laccase-Mediator Systems.” *Bioenergy and Biofuels* 2: 12. doi:10.3389/fenrg.2014.00012.

Ducros, V., A. M. Brzozowski, K. S. Wilson, P. Ostergaard, P. Schneider, A. Svendson, and G. J. Davies. 2001. “Structure of the Laccase from Coprinus Cinereus at 1.68 A Resolution: Evidence for Different ‘Type 2 Cu-Depleted’ Isoforms.” *Acta Crystallographica. Section D, Biological Crystallography* 57 (Pt 2): 333–36.

Durão, Paulo, Isabel Bento, André T. Fernandes, Eduardo P. Melo, Peter F. Lindley, and Lígia O. Martins. 2006. “Perturbations of the T1 Copper Site in the CotA Laccase from Bacillus Subtilis: Structural, Biochemical, Enzymatic and Stability Studies.” *Journal of Biological Inorganic Chemistry: JBIC: A Publication of the Society of Biological Inorganic Chemistry* 11 (4): 514–26. doi:10.1007/s00775-006-0102-0.

Dutton, P. L. 1978. “Redox Potentiometry: Determination of Midpoint Potentials of Oxidation-Reduction Components of Biological Electron-Transfer Systems.” *Methods in Enzymology* 54: 411–35.

Enguita, Francisco J., Lígia O. Martins, Adriano O. Henriques, and Maria Arménia Carrondo. 2003. “Crystal Structure of a Bacterial Endospore Coat Component A LACCASE WITH ENHANCED THERMOSTABILITY PROPERTIES.” *Journal of Biological Chemistry* 278 (21): 19416–25. doi:10.1074/jbc.M301251200.

Forootanfar, Hamid, and Mohammad Ali Faramarzi. 2015. “Insights into Laccase Producing Organisms, Fermentation States, Purification Strategies, and Biotechnological Applications.” *Biotechnology Progress*, October, n/a – n/a. doi:10.1002/btpr.2173.

Frasconi, Marco, Harry Boer, Anu Koivula, and Franco Mazzei. 2010. “Electrochemical Evaluation of Electron Transfer Kinetics of High and Low Redox Potential Laccases on Gold Electrode Surface.” *Electrochimica Acta* 56 (2): 817–27. doi:10.1016/j.electacta.2010.09.056.

Führer, Johannes. 2015. “Directed Evolution of Botrytis Aclada Laccase for Application in Biofuel Cells.”

Heisenberg, Werner, and James MacLachlan. 2009. “Physics and Philosophy: The Revolution of Modern Science. Vol. 19 of World Perspectives.” *Physics Today* 11 (9): 36–38. doi:10.1063/1.3062735.

Ivanov, Ivan, Tanja Vidaković-Koch, and Kai Sundmacher. 2010. “Recent Advances in Enzymatic Fuel Cells: Experiments and Modeling.” *Energies* 3 (4): 803–46. doi:10.3390/en3040803.

Kittl, Roman, Christoph Gonaus, Christian Pillei, Dietmar Haltrich, and Roland Ludwig. 2012. “Constitutive Expression of Botrytis Aclada Laccase in Pichia Pastoris.” *Bioengineered* 3 (4): 232–35. doi:10.4161/bioe.20037.

Kittl, Roman, Kitti Mueangtoom, Christoph Gonaus, Shima Tahvilda Khazaneh, Christoph Sygmund, Dietmar Haltrich, and Roland Ludwig. 2012. “A Chloride Tolerant Laccase from the Plant Pathogen Ascomycete Botrytis Aclada Expressed at High Levels in Pichia Pastoris.” *Journal of Biotechnology* 157 (2): 304–14. doi:10.1016/j.jbiotec.2011.11.021.

Kjaergaard, Christian H., Stephen M. Jones, Sébastien Gounel, Nicolas Mano, and Edward I. Solomon. 2015. “Two-Electron Reduction versus One-Electron Oxidation of the Type 3 Pair in the Multicopper Oxidases.” *Journal of the American Chemical Society* 137 (27): 8783–94. doi:10.1021/jacs.5b04136.

Mate, Diana M., David Gonzalez-Perez, Magnus Falk, Roman Kittl, Marcos Pita, Antonio L. De Lacey, Roland Ludwig, Sergey Shleev, and Miguel Alcalde. 2013. “Blood Tolerant Laccase by Directed Evolution.” *Chemistry & Biology* 20 (2): 223–31. doi:10.1016/j.chembiol.2013.01.001.

McIlvaine, T. C. 1921. “A Buffer Solution for Colorimetric Comparison.” *Journal of Biological Chemistry* 49 (1): 183–86.

Morozova, O. V., G. P. Shumakovich, M. A. Gorbacheva, S. V. Shleev, and A. I. Yaropolov. 2007. “‘Blue’ Laccases.” *Biochemistry (Moscow)* 72 (10): 1136–50. doi:10.1134/S0006297907100112.

Needham, Joseph, Ho Ping-Yu, Lu Gwei-Djen, and Nathan Sivin. 1980. *Science and Civilisation in China: Volume 5, Chemistry and Chemical Technology, Part 4, Spagyrical Discovery and Invention: Apparatus, Theories and Gifts*. Cambridge University Press.

Osipov, Evgeny, Konstantin Polyakov, Roman Kittl, Sergey Shleev, Pavel Dorovatovsky, Tamara Tikhonova, Stephan Hann, Roland Ludwig, and Vladimir Popov. 2014. “Effect of the L499M Mutation of the Ascomycetous Botrytis Aclada Laccase on Redox Potential and Catalytic Properties.” *Acta Crystallographica. Section D, Biological Crystallography* 70 (Pt 11): 2913–23. doi:10.1107/S1399004714020380.

Quintanar, Liliana, Jungjoo Yoon, Constantino P. Aznar, Amy E. Palmer, K. Kristoffer Andersson, R. David Britt, and Edward I. Solomon. 2005. “Spectroscopic and Electronic Structure Studies of the Trinuclear Cu Cluster Active Site of the Multicopper Oxidase Laccase: Nature of Its Coordination Unsaturation.” *Journal of the American Chemical Society* 127 (40): 13832–45. doi:10.1021/ja0421405.

Ramírez, Pablo, Nicolas Mano, Rafael Andreu, Tautgirdas Ruzgas, Adam Heller, Lo Gorton, and Sergey Shleev. 2008. “Direct Electron Transfer from Graphite and Functionalized Gold Electrodes to T1 and T2/T3 Copper Centers of Bilirubin Oxidase.” *Biochimica Et Biophysica Acta* 1777 (10): 1364–69. doi:10.1016/j.bbabio.2008.06.010.

Reinhammar, Bengt R. M., and Tore I. Vänngård. 1971. “The Electron-Accepting Sites in Rhus Vernicifera Lacase as Studied by Anaerobic Oxidation-Reduction Titrations.” *European Journal of Biochemistry* 18 (4): 463–68. doi:10.1111/j.1432-1033.1971.tb01264.x.

Riva, Sergio. 2006. “Laccases: Blue Enzymes for Green Chemistry.” *Trends in Biotechnology* 24 (5): 219–26. doi:10.1016/j.tibtech.2006.03.006.

Roberts, S. A., A. Weichsel, G. Grass, K. Thakali, J. T. Hazzard, G. Tollin, C. Rensing, and W. R. Montfort. 2002. “Crystal Structure and Electron Transfer Kinetics of CueO, a Multicopper Oxidase Required for Copper Homeostasis in Escherichia Coli.” *Proceedings of the National Academy of Sciences* 99 (5): 2766–71. doi:10.1073/pnas.052710499.

Schafee, Thomas. 2015. “Directed Evolution.” *Wikipedia, the Free Encyclopedia*.

Shi, Song, Yujuan Wang, Aihua Xu, Huajun Wang, Dajian Zhu, Suparna Baksi Roy, Timothy A. Jackson, Daryle H. Busch, and Guochuan Yin. 2011. “Distinct Reactivity Differences of Metal Oxo and Its Corresponding Hydroxo Moieties in Oxidations: Implications from a manganese(IV) Complex Having Dihydroxide Ligand.” *Angewandte Chemie (International Ed. in English)* 50 (32): 7321–24. doi:10.1002/anie.201100588.

Shleev, Sergey, Viktor Andoralov, Magnus Falk, Curt T. Reimann, Tautgirdas Ruzgas, Martin Srnec, Ulf Ryde, and Lubomír Rulíšek. 2012. “On the Possibility of Uphill Intramolecular Electron Transfer in Multicopper Oxidases: Electrochemical and Quantum Chemical Study of Bilirubin Oxidase.” *Electroanalysis* 24 (7): 1524–40. doi:10.1002/elan.201200188.

Shleev, Sergey, Anna Jarosz-Wilkolazka, Anna Khalunina, Olga Morozova, Alexander Yaropolov, Tautgirdas Ruzgas, and Lo Gorton. 2005. “Direct Electron Transfer Reactions of Laccases from Different Origins on Carbon Electrodes.” *Bioelectrochemistry (Amsterdam, Netherlands)* 67 (1): 115–24. doi:10.1016/j.bioelechem.2005.02.004.

Shleev, Sergey, Curt T. Reimann, Vladimir Serezhenkov, Dosymzhan Burbaev, Alexander I. Yaropolov, Lo Gorton, and Tautgirdas Ruzgas. 2006. “Autoreduction and Aggregation of Fungal Laccase in Solution Phase: Possible Correlation with a Resting Form of Laccase.” *Biochimie* 88 (9): 1275–85. doi:10.1016/j.biochi.2006.02.007.

Solomon, Edward I., Uma M. Sundaram, and Timothy E. Machonkin. 1996. “Multicopper Oxidases and Oxygenases.” *Chemical Reviews* 96 (7): 2563–2606.

Sucheta, A., R. Cammack, J. Weiner, and F. A. Armstrong. 1993. “Reversible Electrochemistry of Fumarate Reductase Immobilized on an Electrode Surface. Direct Voltammetric Observations of Redox Centers and Their Participation in Rapid Catalytic Electron Transport.” *Biochemistry* 32 (20): 5455–65.

Wilson, G. S. 1978. “Determination of Oxidation-Reduction Potentials.” *Methods in Enzymology* 54: 396–410.

Xu, F. 1997. “Effects of Redox Potential and Hydroxide Inhibition on the pH Activity Profile of Fungal Laccases.” *The Journal of Biological Chemistry* 272 (2): 924–28.

Xu, F. 2001. “Dioxygen Reactivity of Laccase: Dependence on Laccase Source, pH, and Anion Inhibition.” *Applied Biochemistry and Biotechnology* 95 (2): 125–33.

Xu, F., A. E. Palmer, D. S. Yaver, R. M. Berka, G. A. Gambetta, S. H. Brown, and E. I. Solomon. 1999. “Targeted Mutations in a Trametes Villosa Laccase. Axial Perturbations of the T1 Copper.” *The Journal of Biological Chemistry* 274 (18): 12372–75.